Report 3677

DRAG REDUCTION AND DEGRADATION OF DILUTE POLYMER SOLUTIONS IN TURBULENT PIPE FLOWS

NAVAL SHIP RESEARCH AND DEVELOPMENT CENTER
Washington, D. C. 20034

DRAG REDUCTION AND DEGRADATION OF DILUTE POLYMER SOLUTIONS IN TURBULENT PIPE FLOWS

by

T. T. Huang and N. Santelli

APPROVED FOR PUBLIC RELEASE: DISTRIBUTION UNLIMITED

SHIP PERFORMANCE DEPARTMENT
RESEARCH AND DEVELOPMENT REPORT

August 1971

Report 3677

The Naval Ship Research and Development Center is a U.S. Navy center for laboratory effort directed at achieving improved sea and air vehicles. It was formed in March 1967 by merging the David Taylor Model Basin at Carderock, Maryland and the Marine Engineering Laboratory (now Naval Ship R & D Laboratory) at Annapolis, Maryland. The Mine Defense Laboratory (now Naval Ship R & D Laboratory) Panama City, Florida became part of the Center in November 1967.

Naval Ship Research and Development Center
Washington, D.C. 20034

MAJOR NSRDC ORGANIZATIONAL COMPONENTS

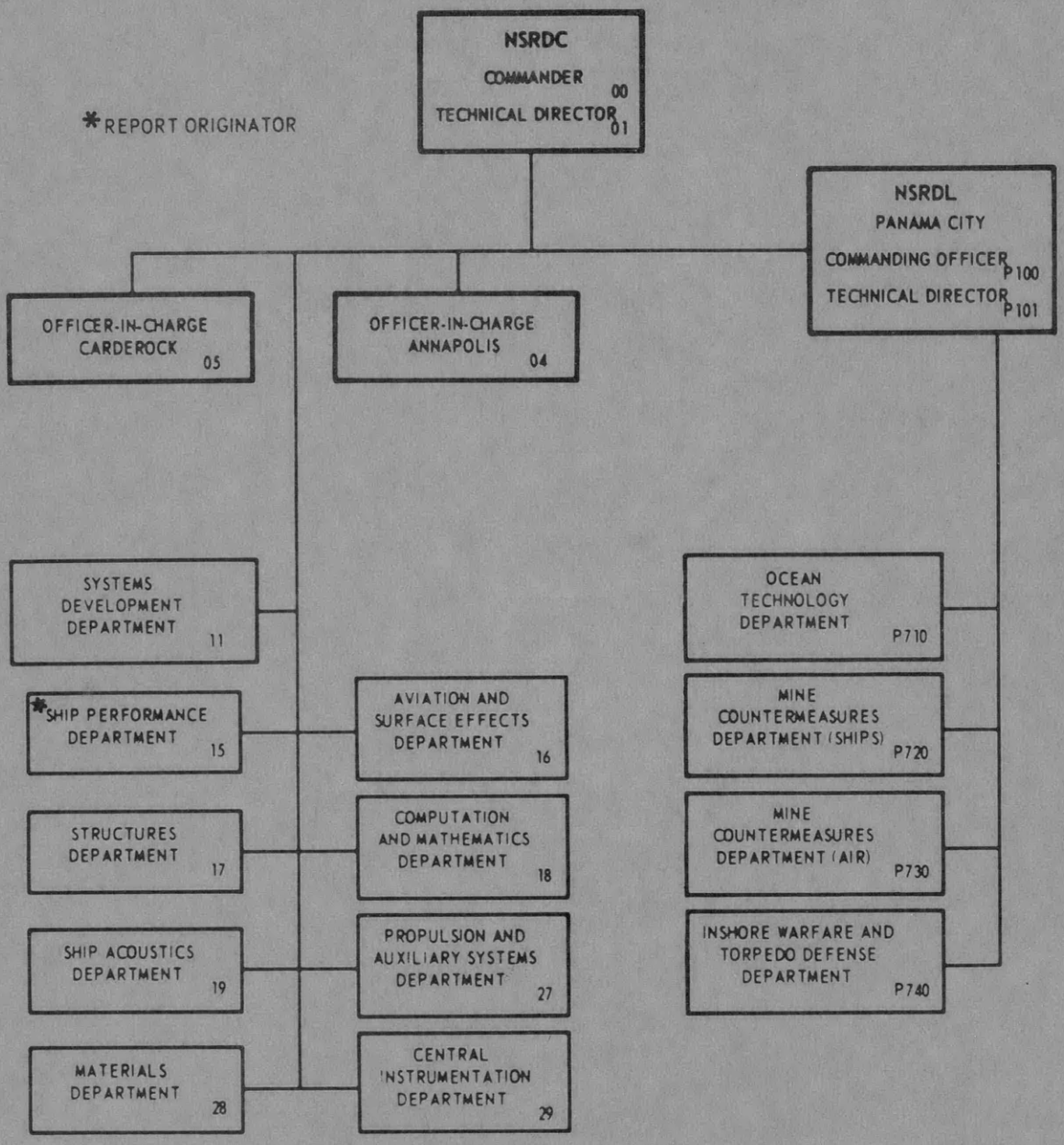

NDW-NSRDC 3960/43 (3-70)

DEPARTMENT OF THE NAVY
NAVAL SHIP RESEARCH AND DEVELOPMENT CENTER
WASHINGTON, D. C. 20034

DRAG REDUCTION AND DEGRADATION OF DILUTE POLYMER SOLUTIONS IN TURBULENT PIPE FLOWS

by

T. T. Huang and N. Santelli

August 1971 Report 3677

TABLE OF CONTENTS

LIST OF FIGURES

NOTATION

A	Slope of logarithmic velocity law in common logarithms for ordinary Newtonian fluid or (2.3026)/K
$\tilde{A}$	Slope of logarithmic velocity law in common logarithms for the strongly interactive layer, Equation (1b)
B	Constant of the ordinary Newtonian inner logarithmic velocity law, Equation (1c)
$\tilde{B}$	Constant of the modified inner logarithmic velocity law, Equation (1b)
ΔB	Constant defined in Equation (5)
$\Delta\tilde{B}$	Constant defined in Equation (2)
C	Concentration of polymer solution
D	Diameter of pipe
f	Darcy-Weibach friction factor
K	Von Kármán constant
ℓ	Length parameter for polymer solution
M_w	Weight-average of molecular weight of polymer solution
Q_T	Torque measured by viscometer
$R = VD/\nu$	Reynolds number
R_c	Radius of the cone in viscometer
R_g	Radius of gyration of polymer molecules in angstroms
$\hat{r}$, $\hat{z}$, $\hat{\theta}$	Cylindric coordinates defined in Figure 1
U_{max}	Maximum velocity at pipe axis
u	Local mean/velocity
$u_\tau = \sqrt{\tau_w/\rho}$	Shear velocity
$u^+ = u/u_\tau$	Nondimensional mean velocity
V	Average velocity across pipe cross section
V_p	Average velocity for polymer-solvent system

V_s	Average velocity for solvent alone
ΔV^+	$= \{V_p/u_\tau - V_s/u_\tau\}$ at constant u_τ, drag reduction function corresponding to traditional ΔB
ΔV^+_{max}	Saturated value of ΔV^+
y	Normal distance from the wall
$y^+ = u_\tau y/\nu$	Nondimensional distance from the wall
y_ℓ	Thickness of laminar sublayer
$y^+_\ell = u_\tau y_\ell/\nu$	Nondimensional thickness of laminar sublayer
y_s	Thickness of strongly interactive layer
$y^+_s = u_\tau y_s/\nu$	Nondimensional thickness of strongly interactive layer
y_w	Thickness of weakly interactive layer
$y^+_w = u_\tau y_w/\nu$	Nondimensional thickness of weakly interactive layer
dp/dx	Pressure gradient along pipe
$\dot{\alpha}$	Angular velocity of viscometer
$\dot{\gamma}$	Strain rate
$[\eta]$	Steady state intrinsic viscosity
θ	Angle between the cone and the plate of viscometer
μ	Dynamic viscosity of the fluid
μ_p	Dynamic viscosity of polymer-solvent system
μ_s	Dynamic viscosity of solvent alone
ν	Kinetic viscosity of the fluid
$\S = y/(D/2)$	Nondimensional y
$\S_\ell = y_\ell/(D/2)$	Nondimensional y_ℓ
$\S_s = y_s/(D/2)$	Nondimensional y_s
ρ	Mass density of the fluid
$\sigma_{z\theta}$	Shear stress
τ_w	Wall shear stress

ABSTRACT

Drag reduction caused by dilute Polyethylene Oxide (POLYOX WSR-301) and anionic charged Polyacrylimide (MAGNIFLOC 835A) polymer solutions was studied experimentally in 1.918- and 0.455-cm ID smooth pipes. The POLYOX solutions tested are superior in drag reduction but inferior in shear-degradation resistance compared to the MAGNIFLOC solutions at corresponding concentrations. A three-layer mean velocity profile model appears to be more consistent with current and other data than a traditional two-layer model. Drag reduction properties measured in terms of $\Delta V^+ = (V_p/u_\tau) - (V_s/u_\tau)$, which corresponds to the traditional ΔB, depends strongly on pipe diameter and ΔV^+ departs from the linear-logarithmic Meyer relationships at high wall shear stresses. The onset of measured drag reduction depends upon solution concentration and is seriously affected by shear degradation.

ADMINISTRATIVE INFORMATION

This work was sponsored by the Naval Ship Systems Command and was funded under Subproject SF354 21 003, Task 01710.

INTRODUCTION

Drag reduction by longchain, high molecular weight additives was first reported by Toms.[1] Explanation was attempted at the same time by Oldroyd,[2] who postulated that the mechanism responsible for drag reduction was a thin slip layer formed near the wall boundary. During the sixties, investigators renewed interest in drag-reducing polymer solutions because of their merit in solving engineering problems, such as increasing flow rates in pipe lines and increasing ship speed. Most experimental studies so far have been made in turbulent, smooth, pipe flow facilities. Data reported in the literature may be classified in two main groups: (1) the gross flow measurements of pressure drop versus flow rate, such as the work of Wells,[3] Savins,[4] Ernst,[5] Elata and Tirosh,[6] Fabula,[7] Virk et al.,[8] Hershey and Zakin,[9] Van Driest,[10] and Paterson and Abernathy;[11] and (2) the mean velocity profile measurements during drag reduction, e.g., data of

---

[1]References are listed on page 31.

Elata et al.,[12] Ernst,[5] Virk et al.,[8] Goren and Norburg,[13] Wells et al.,[14] Patterson and Florez,[15] Tomita,[16] Seyer and Metzner,[17] and Tsai.[18] A few measurements of the structure of turbulence during drag reduction were made by Virk et al.,[8] Wells et al.,[14] and Seyer and Metzner.[17] However, the results are as yet inconclusive.

Meyer[19] used velocity similarity laws with a negative roughness analogy to interpret the early experimental data.[15,16] His concept was determined by the fact that a semilogarithmic plot of velocity profiles for drag-reducing fluids showed a parallel upward shift, compared to Newtonian fluids; see Reference 5. This implied that the von Kármán constant K in the semilogarithmic similarity laws was not altered by the polymer solutions, and the only change was in the numerical constant B in the inner similarity law, resulting from the sublayer thickening. Meyer found that the change of B occurred only above a critical shear stress and was a function of shear stress and solution concentration, independent of pipe diameter. These phenomenological analyses, called the Meyer correlations, seem to interpret the data of Ernst[5] (CMC solutions), Wells,[3] and Elata et al.[6,12] (Guar gum solutions). Unfortunately, the polymer solutions studied were at low drag-reducing fluids. The analysis by Seyer and Metzner[17] was parallel to the Meyer correlations except that a relaxation time parameter was introduced to generalize a relationship for the change of B. However, the model in which the constant B was shifted failed gradually with increasing drag reduction. Van Driest[10] was the first to propose the need for changing the Von Kármán constant near the wall and to postulate a three-layer model. Virk et al.[20] and Virk[21] by himself further elaborated the three-layer model.

The mechanism responsible for drag reduction is still not understood, and interpreting gross flow data through velocity similarity laws is not fully agreed upon. Nevertheless, the recent velocity profile measurements of Tsai[18] and Seyer and Metzner[17] confirm the three-layer model, except that the numerical constants in the middle layer are slightly different from those proposed by Van Driest[10] and Virk et al.[20] From the two groups of data, however, gross flow and velocity profile information appear to have emerged. The mean velocity profile in the inner region of the turbulent boundary layer during drag reduction may be divided into (1) a viscous

sublayer, similar to Newtonian; (2) a strongly interactive layer, characterized by a small Von Kármán constant; and (3) a weakly interactive, characterized by changing the constant B but not the Von Kármán constant. On the basis of the three-layer model, the gross flow may be classified according to three regimes: (1) without drag reduction; (2) with drag reduction, depending upon the hydrodynamic and polymeric characteristics of the polymer-solvent system; and (3) a saturated region, limiting the maximum drag reduction attainable by all polymer solutions. For Regime 1, the strongly interactive layer is absent, the weakly interactive layer is the same as that for a Newtonian fluid. For Regime 3 the strongly interactive layer dominates the entire interactive zone. The three layers are present in Regime 2. In Regime 2 it is essential to obtain the relationship between the thickness of the strongly interactive layer and the hydrodynamic and polymeric characteristics of the polymer-solvent system such as polymer concentration, polymer length and time scale, wall shear stress, and pipe diameter. It becomes apparent that the Meyer[19] correlations are satisfactory for low drag-reducing fluids since the strongly interactive layer is rather thin. It is expected that the strongly interactive layer will become thicker with increasing drag reduction; thus, the Meyer correlation fails progressively with increasing drag reduction.

Experimental data collected so far are mostly limited to low shear stresses at $<10^3$ dyn/cm^2, and low Reynolds numbers, $<10^5$. Many potential applications for drag-reducing polymer solutions, such as for fire hoses and ship boundary layers, are not covered in the range of available data. The primary objective of this study is to evaluate the application of the three-layer velocity-similarity laws to the highly effective drag-reducing polymer solutions. The validity of these laws at high shear stresses and high Reynolds numbers will be stressed. The Virk[8] report on the onset of drag reduction, which is contradictory to the results of White,[22] Spangler,[23] Van Driest,[10] and Paterson and Abernathy,[11] will be examined.

Many analytical works[24-27] have been developed for predicting characteristics of the external boundary layer in polymer solutions. Most of them adopted the Meyer corrections.[19] Thus, the results of these analyses when applied to high drag-reducing polymer solutions may be in error.

The present study discusses only the flow of a fresh homogeneous polymer solution on a smooth boundary. The effect of solution degradation on the drag reduction is briefly studied; however, the complication of roughness and diffusion after injection is not included.

POLYMER SOLUTION PREPARATION

Two very effective drag-reducing polymers are used in this study. One is POLYOX WSR-301, blend 8259W, which is a polyethylene oxide product of Union Carbide Corporation. The other is MAGNIFLOC 835A, an anionic charged polyacrylimide product of American Cyanamid Co. Throughout this study, polymer solutions were prepared by mixing the dry polymer powder in distilled water to a concentration of 1000 ppm. After being stirred gently for about an hour, the 1000 ppm solution remained undisturbed overnight and then, just before the experiments, was diluted with well water to various concentrations.

POLYMER SOLUTION PROPERTIES

The steady state intrinsic viscosity is a parameter often used to estimate the molecular weight, radius of gyration, and relaxation-time parameter of polymer solutions. The intrinsic viscosity was measured directly by a Well-Brookfield micro viscometer. The tested polymer solution of 1 cc was placed between a cone and a plate as sketched in Figure 1. The cone was rotated at a constant speed, while the torque of the cone, which was directly proportional to the viscosity of the solution, was measured by a torque-spring meter, i.e.,

$$\mu = \frac{\sigma_{z\theta}}{\dot{\gamma}_{z\theta}} = \frac{3\dot{\alpha}Q_T}{2\pi R_c^3\theta} \quad (\text{for } \theta < 3°)$$

where μ is the dynamic viscosity; $\sigma_{z\theta}$ is the shear stress; $\dot{\gamma}$ is the strain rate (velocity gradient); $\dot{\alpha}$ is the angular velocity; Q_T is the torque; R_c is the radius of the cone; and θ is the angle between the cone and the plate. The advantage of using this type of viscometer is that the strain rate is uniform throughout the volume if θ is less than 3 deg. The temperature of the solution was controlled by circulating water from a

constant temperature bath through the bottom of the plate. The steady-state intrinsic viscosity of polymer solution is defined as

$$[\eta] = \lim_{\substack{\dot{\gamma}\to 0 \\ C\to 0}} \frac{\frac{\mu_p(\dot{\gamma})}{\mu_s} - 1}{C}$$

where $\mu_p(\dot{\gamma})$ is the polymer solution viscosity; μ_s is solvent viscosity at the same temperature; C is polymer concentration in grams per deciliter (g/dl); and $\dot{\gamma}$ is the strain rate in seconds. The effect of viscometer strain rate on the value of $(\mu_p/\mu_s - 1)/C$ for POLYOX WSR-301 at 25 C is shown in Figure 2; for MAGNIFLOC 835A, in Figure 3. Both figures show significant strain-rate dependence upon measured $(\mu_p/\mu_s - 1)/C$. The steady-state measured intrinsic viscosity of the two polymer solutions is obtained by extrapolating from the values of $\lim_{\dot{\gamma}\to 0} (\mu_p/\mu_s - 1)/C$ to $C \to 0$ as shown in Figures 4 and 5. The degraded POLYOX solution in Figure 4 was obtained by recirculating the 1000-ppm fresh solution through a pump for 1/2 hour. An order of magnitude reduction in intrinsic viscosity was detected after applying this violent agitation to the POLYOX solution. The same violent agitation was applied to the MAGNIFLOC 835A solution but measured intrinsic viscosity showed no noticeable change. The relationship of stress versus strain rate at various concentrations for the two polymer solutions is given in Figures 6 and 7. POLYOX solutions behave like Newtonian fluids for concentrations less than 500 ppm. Within this range the polymer viscosity can be approximated by

$$\mu_p = \mu_s \{1 + [\eta]\, C + 0.4\, [\eta]^2\, C^2\}$$

which is in agreement with Shin[28] and Paterson and Abernathy.[11] As shown in Figure 7, significant non-Newtonian behavior (shear thinning) is noticed for MAGNIFLOC 835A solutions, although it appears the solutions may have a Newtonian range at sufficiently high shear rates.

According to Merrill et al.,[29] the average molecular weight and radius of gyration of POLYOX solutions can be expressed as a function of intrinsic viscosity, i.e.,

$$[\eta] = (1.03 \times 10^{-4}) M_w^{0.78}$$

and

$$R_g = 367 [\eta]^{0.65}$$

where M_w is the weight-average of molecular weight given in grams per gram mole, and R_g is the radius of gyration in angstroms. Since the measured steady-state intrinsic viscosity is 16.5 dl/gm for the present fresh POLYOX WSR-301 solutions, the weight-average molecular weight is 5×10^6 and the radius of gyration is about 2300 A. If the Merrill relationship is used for the present degraded POLYOX solution (the relationship is questionable since the degradation will cause drastic change in the spectrum of molecular weight), the present degradation treatment will result in a reduction of average molecular weight from 5×10^6 to 2.5×10^5 and reduction of radius of gyration from 2300 to 520 A. The molecular weight quoted by the MAGNIFLOC manufacturer is 15×10^6, compared to 16×10^6 predicted by the Merrill relationship. The comparison is quite good. The radius of gyration for MAGNIFLOC 835A is 4000 A if the Merrill relationship is used.

GROSS-FLOW MEASUREMENTS

A flow facility consisting of a 1.918-cm ID smooth brass pipe with a wall thickness of 1.6 mm was built and tested to provide needed gross flow data of very high drag-reducing polymer solutions at high shear stress and high Reynolds number. In addition, a 0.455-cm ID, smooth copper pipe with a wall thickness of 0.9 mm was used to study the pipe-diameter effect. The test pipes were about 10 m long and inside surfaces of the pipes were polished carefully. Since the drag-reduction properties of dilute polymer solutions are sensitive to mechanical degradation, it was decided to use a single-pass blowdown pipe-flow apparatus. Figure 8 shows the overall

experimental setup and associated instrumentation. A large head tank holding 800 liters was connected to the two vertical test pipes; the flow rate to the pipes was regulated by varying the air pressure at the head tank. Testing was done by forcing the polymer solutions through the instrumented length of test pipe into a weighing barrel, after which the solution was discarded. Two controlling ball valves were located at the downstream ends of the pipes to avoid solution degradation. Smooth abrupt inlets were used to encourage transition from laminar to turbulent flow soon after the inlet. The sharp edges of the inlets were carefully smoothed out to minimize mechanical degradation of the solutions. At 120 diameters downstream from the inlet, the pipes were instrumented with four static pressure taps. The pressure drops along the lengths of the pipes were measured by Pace differential pressure gages. Signals from the gages were averaged electronically for 10 sec and were then displayed by digital voltmeters. The shortest run time was about 40 sec for cases at the highest speed. Most run times were kept about 120 sec to allow sufficient time for measuring accurate flow rates at the weighing barrel. The pressure drops presented here are the average values of the measurements of the three length intervals between the four pressure taps on each pipe. The discrepancies between the three readings are less than 3 percent. The error involved in repeating an identical run was less than 5 percent. High quality control was maintained by carefully mixing and transferring the tested dilute polymer solution. Degradation of drag-reduction properties of each polymer along the lengths of the pipes was found to be less than the experimental accuracy. Thus, the turbulent flow in the pipes was fully developed, and the shear degradation of the solutions along the pipes was not serious. The only possible shear degradation to which the fluid was subjected before the instrumented lengths was at the inlets. The temperature of the solutions during the tests was 73 ± 3 F.

THREE-LAYER MEAN VELOCITY PROFILE

The recent experimental mean velocity profiles obtained by Seyer and Metzner[17] and Tsai[18] at high drag-reduction rates are plotted in Figure 9. These data are an excellent confirmation of the three-layer model proposed first by Van Driest[10] and later by Virk et al.[20,21]

On the basis of Figure 9, the nondimensional profile for the three layers can be expressed as a

1. Laminar Sublayer ($0 \leq y \leq y_\ell$)

$$u^+ = \frac{u}{u_\tau} = \frac{u_\tau y}{\nu} = y^+; \; 0 \leq y^+ \leq y_\ell^+ \tag{1a}$$

2. Strongly interactive layer ($y_\ell \leq y \leq y_s$)

$$u^+ = \tilde{A} \log y^+ + \tilde{B}; \; y_\ell^+ \leq y^+ \leq y_s^+ \tag{1b}$$

3. Weakly interactive layer ($y_s \leq y \leq y_w$)

$$u^+ = A \log y^+ + B + \Delta\tilde{B}; \; y_s^+ \leq y^+ \leq y_w^+ \tag{1c}$$

where u is the mean velocity; u_τ is the friction velocity in $\sqrt{\tau_w/\rho}$, where τ_w is the wall shear stress, and ρ is the mass density of the fluid; y is the distance from the wall; and ν is the kinematic viscosity of the fluid. The overlapping zone between the inner and outer velocity similarity laws is almost valid from the laminar sublayer to the pipe axis for the ordinary Newtonian turbulent pipe flow.[30] Thus, the error introduced by using either the inner or the outer law alone throughout the pipe cross section is known to be small. The same argument is assumed valid for drag-reducing polymer pipe flows. Furthermore, since data shown in Figure 9 cover the entire cross section, the modified inner law is valid up to the pipe axis. Thus, the outer edge of the weakly interactive layer may be assumed equal to D/2. Nevertheless, the same results may be obtained by using the corresponding outer laws of the form

$$\frac{U_{max} - u}{u_\tau} = - A \log \left(y/(D/2) \right)$$

for $y_s \leq y \leq D/2$. The subscripts ℓ, s, and w represent the thicknesses of the laminar sublayer and the strongly and weakly interactive layers, respectively. The difference between the present study and others[10,20,21]

is in the selection of the constants $\tilde{A}$ and $\tilde{B}$. The present study is based on the best fit of data shown in Figure 9, i.e. $\tilde{A} = 30$, $\tilde{B} = -20.2$, while Van Driest[10] selected $\tilde{A} = 27$, $\tilde{B} = -17.2$, and Virk et al.[20] used $\tilde{A} = 26.9$, $\tilde{B} = -17$. They obtained these constants from the interpretation of gross-flow measurements. The two constants A and B are taken from data of the ordinary Newtonian flow, i.e., $A = 5.75$ and $B = 5.5$. At the two intersections of the three layers, the velocity has to be continuous; thus ΔB can be expressed as a function y_s and y_ℓ, using Equations (1a,b,c), i.e.,

$$\Delta\tilde{B} = \tilde{A} \log \left(\frac{y_s^+}{y_\ell^+}\right) - A \log y_s^+ - B + y_\ell^+ \tag{2}$$

By definition, the average velocity V across the pipe cross section is

$$V = \frac{Q}{\pi D^2/4} = \int_0^1 u \, d\,(1 - \S)^2 \tag{3}$$

where Q is the flow rate, $\S = y/(D/2)$, and D is the pipe diameter. The integration of Equation (3) through the three layers, using Equations (1a,b,c), can be evaluated readily to give,

$$\begin{aligned}\frac{V}{u_\tau} = {} & A \log \frac{D/2u_\tau}{\nu} + B + \Delta\tilde{B} - \frac{3}{2}\left(\frac{A}{2.3026}\right) \\ & - \frac{2}{2.3026}(\tilde{A} - A)\left(\S_s - \frac{\S_s^2}{4}\right) \\ & + \left\{\frac{D/2u_\tau}{\nu}\left(\S_\ell^2 - \frac{2}{3}\S^3\right) + \frac{2\tilde{A}}{2.3026}\left(\S_\ell^2 - \frac{\S_\ell^3}{4}\right) - \frac{y_\ell u_\tau}{\nu}\left(2\S_\ell^2 - \S_\ell^3\right)\right\}\end{aligned} \tag{4}$$

where $\Delta\tilde{B}$ is given in Equation (2). Equation (4) is the primary result of the dimensional analysis for the three-layer model and forms the framework for interpreting the gross-flow data in the following sections. It is noted that if the strongly interactive layer is neglected, then Equation (4)

reduces to a form similar to those obtained by other investigators, i.e.,[5,7,12,17,19]

$$\frac{V}{u_\tau} = A \log \frac{D/2u_\tau}{\nu} + B + \Delta B - \frac{3}{2}\left(\frac{A}{2.3026}\right) + \{\ \} \qquad (5)$$

where $\Delta B = y_\ell^+ - (A \log y_\ell^+ + B)$ and $\{\ \}$ is the last bracket in Equation (4). It is apparent that ΔB increases with increasing thickness of the laminar sublayer for polymer solutions ($y_\ell^+ > 11.6$). In past studies, the main effort has been to relate ΔB or y_ℓ^+ to the characteristics of the drag-reducing system,[5,7,12,17,19] using Equation (5). However, these approaches could not be used to interpret the saturated drag reduction line (see next section), which is commonly observed[7,8,11,20,21] and is not in agreement with data shown[17,18] in Figure 9. The three-layer model, which includes a strongly interactive layer, appears to be more general and closer to reality.

SATURATED DRAG-REDUCTION LINE

The drag reduction for high drag-reducing polymer solutions often reaches a saturation limit above which further increases of polymer concentration produce no further drag reduction. This phenomenon was first reported by Fabula[7] and by Hoyt and Fabula.[31] Virk et al.[8,20,21] were the first to study the phenomenon in detail. Thus it was often called the Virk maximum drag-reduction asymptote. We will assume that for the case of saturated drag reduction the strongly interactive layer dominates the entire pipe (the weakly interactive layer is absent); then by integrating Equation (3) through the two layers, Equation (4) becomes

$$\frac{V}{u_\tau} = \tilde{A} \log \left(\frac{D/2u_\tau}{\nu}\right) + \tilde{B} - \frac{3}{2}\left(\frac{\tilde{A}}{2.3026}\right) + \{\ \}, \text{ as } \S_s \to 1$$

$$= 30 \log \left(\frac{Du_\tau}{\nu}\right) - 48.8 \qquad (6)$$

Here we use A = 30, B = -20.2. The $\{\ \}$ term is the last bracket in Equation (4), which is much smaller than the other terms in Equations (4)

and (6), and will be neglected for deriving the friction factor. The Darcy-Weibach friction factor can then be written as

$$\frac{1}{\sqrt{f}} = \frac{\tilde{A}}{\sqrt{8}} \log (R\sqrt{f}) + \frac{\tilde{B} - \left(\frac{3}{2} + \frac{1}{2} \log 32\right) \tilde{A}}{\sqrt{8}} \tag{7}$$

where $R = DV/\nu$, the Reynolds number, and $f = 8\tau_w/(\rho V^2)$. Substituting the best-fit values for A and B (A = 30, B = -20.2) from Figure 9, the saturated drag reduction line has the form

$$\frac{1}{\sqrt{f}} = 10.6 \log (R\sqrt{f}) - 22 \tag{8}$$

which is in between the first[8] and second[20] Virk formulas (shown in Figure 10), i.e.

$$\frac{1}{\sqrt{f}} = 11.5 \log (R\sqrt{f}) - 25$$

and

$$\frac{1}{\sqrt{f}} = 9.5 \log (R\sqrt{f}) - 19$$

Further experimental evidence of the saturated drag-reduction line based on the present study is shown in Figure 10. The present derived formula, Equation (8), appears to fit the data better than Virk's two formulas, especially at high shear stresses and high Reynolds numbers. It is interesting to note that the modified Von Kármán constant K of Equation (6), corresponding to A = 30, is 0.077, which is about one-fifth of the Newtonian value K = 0.4. Since the derived saturated drag reduction line is in good agreement with experimental data, the assumption that the strongly interactive layer dominates the entire pipe for the case of saturated drag reduction is valid.

DISCUSSION OF PRESENT GROSS-FLOW DATA

The measured gross-flow drag-reduction data are plotted in various forms in Figures 11-24. The measured Darcy friction factor, $f = 8\tau_w/(\rho V^2) = 2D(dp/dx)/(\rho V^2)$, versus Reynolds number ($R = VD/\nu$) for POLYOX WSR-301 solutions is shown in Figure 11, and the factor for MAGNIFLOC 835A solutions is given in Figure 12, where dp/dx is the pressure gradient along the pipe. The plot of $1/\sqrt{f}$ versus $R\sqrt{f}$ for POLYOX solutions is shown in Figure 13, and that for MAGNIFLOC solutions is shown in Figure 14. Figures 15 and 16 display V/u_τ versus u_τ/ν for POLYOX solutions tested in 0.455- and 1.918-cm pipes, respectively. The data of Virk et al.[8] and Paterson and Abernathy[11] are also shown in Figures 15 and 16 for comparison. The reason for using a dimensional parameter u_τ/ν here rather than a more complete nondimensional parameter used by Granville[24] (i.e. $u_\tau \ell/\nu$) is due to the fact that the appropriate characteristic length parameter ℓ for polymer solutions has not yet been agreed upon. Nevertheless, a suitable ℓ may be inserted in the figures without difficulty whenever it is available. It is noted that the pipe diameter used by Paterson and Abernathy[11] is 1.742 cm, which is close to the 1.918-cm pipe, and the two results shown in Figure 16 are very close to each other although the measured values of steady-state intrinsic viscosity are different owing to different measuring techniques. A serious effect of shear degradation at inlet on drag reduction measured by small pipes was reported by Virk et al.[8] (D = 0.292 cm) and by Paterson and Abernathy[11] (D = 0.63 cm). The present small pipe (D = 0.455 cm) for testing POLYOX solutions may suffer some degree of shear degradation, since the present inlet does not use a bell-mouth entrance, although the sharp edges at the inlet are smoothed out. For MAGNIFLOC solutions this effect is less serious because the solutions have stronger resistance to shear degradation (see next section). Figures 17 and 18 show the V/u_τ versus u_τ/ν for MAGNIFLOC solutions.

We may further define a parameter

$$\Delta V^+ = \left\{ \frac{V_p}{u_\tau} - \frac{V_s}{u_\tau} \right\} \text{ at constant } u_\tau$$

where the subscripts p and s represent the polymer-solvent system and solvent alone, respectively. It may be noted that ΔV^+ is equal to the traditional ΔB as discussed by McCarthy.[25] According to Equation (4), ΔV^+ may be written as

$$\Delta V^+ = \Delta\tilde{B} - \frac{2}{2.0326}(\tilde{A} - A)\left(\S_s - \frac{\S_s^2}{4}\right)$$

$$= (\tilde{A} - A)\left\{\log\left(\frac{y_s^+}{y_\ell^+}\right) - \frac{2}{2.3026}\S_s\left(1 - \frac{\S_s}{4}\right)\right\}$$

$$+ y_\ell^+ - A \log y_\ell^+ - B \qquad (9)$$

where the difference is assumed to be small between the laminar sublayer thickness of solvent and polymer-solvent system, and the quantity $\{\ \}_p - \{\ \}_s$ from (4) has been neglected. At the saturated drag reduction ΔV^+ is

$$\Delta V^+_{max} = (\tilde{A} - A)\log\frac{Du_\tau}{\nu} - (\tilde{A} - A)\left(\log y_\ell^+ + \frac{3}{4.6052} + \log 2\right)$$

$$= 24.25 \log\frac{Du_\tau}{\nu} - 48.9 \qquad (10)$$

where y_ℓ^+ is assumed equal to 11.6. If we use the Von Kármán-Prandtl resistance equation for the solvent, i.e.

$$\frac{1}{\sqrt{f}} = 2 \log (R\sqrt{f}) - 0.8 \qquad (11)$$

then V_s/u_τ is

$$\frac{V_s}{u_\tau} = 5.657 \log\frac{Du_\tau}{\nu} + 0.292$$

Thus, Equation (7) becomes

$$\Delta V^+_{max} = 24.34 \log \frac{Du_\tau}{\nu} - 48.5 \qquad (12)$$

The difference between Equations (10) and (12) is small, and Equation (12) will be used for ΔV^+_{max}. The measured ΔV^+ versus u_τ/ν for POLYOX solutions is plotted in Figure 19 and that for MAGNIFLOC solutions is in Figure 20. The comparison of the present measured ΔV^+ data with those obtained by Fabula[7] (D = 1.02 cm) is shown in Figure 21. The summary of the present measured ΔV^+ data at wall shear stresses τ_w = 500, 1000, and 1500 dyn/cm^2 and at 75 F for POLYOX and MAGNIFLOC solutions is plotted against concentration in Figure 22. The effect of pipe diameter on measured ΔV^+ data for POLYOX solutions is displayed in Figure 23.

As shown in Figures 11-18, the measured drag-reduction data for dilute POLYOX and MAGNIFLOC solutions lie between the solvent curve (Equation (11)) and the derived saturated drag-reduction line as given in Equation (7). During high drag reduction (close to the saturated drag-reduction line), all the slopes of the measured curves shown in Figures 11-18 are found to be parallel to the slopes of the saturated line. However, with decreasing drag reduction the slopes of measured curves deviate progressively from those of the saturated line and become closer to those of the solvent curves.

As shown in Figures 19 and 20, the values of ΔV^+ increase linearly with increasing values of log (u_τ/ν) when u_τ/ν exceeds the onset of drag reduction. However, the increase of ΔV^+ levels off at $u_\tau/\nu \approx 2 \times 10^3$ (cm^{-1}) and finally drops off at $u_\tau/\nu \approx 3 \times 10^3$ cm^{-1}. The value of u_τ/ν = 2×10^3 cm^{-1} corresponds to wall shear stresses of 1280 dyn/cm^2 at 32 F, 340 dyn/cm^2 at 75 f, and 130 dyn/cm^2 at 120 F. It is apparent that many practical applications are in the region of $u_\tau/\nu > 2 \times 10^3$ cm^{-1}. Unfortunately, data are rather scarce in this region.

Meyer,[19] Elata,[12] and Virk et al.[8] found that dilute polymer solutions produced no drag reduction until the wall shear stress exceeded a critical value, and this value was found to be independent of polymer concentration and pipe diameter. Virk et al. found that this critical value depended upon the ratio of a turbulent wall length scale, and the radius of gyration of the polymer molecule in solution R_g, i.e.,

$$\frac{2R_g u_\tau}{\nu} = \text{onset constant (0.015)} \qquad (13)$$

Figures 19 and 20 show the onset of drag reduction in the present study for various concentrations of POLYOX WSR-301 and MAGNIFLOC 835A solutions tested in both pipes. The point of onset is seen to move to higher values of wall shear stress as the concentration decreases. The onset of drag reduction of the dilute polymer solution is also dependent upon the pipe diameter. For examples, the Virk onset constants for the fresh POLYOX solutions measured by the 1.918-cm pipe are 0.0066, 0.0044, and 0.002 at 5, 10, and 50 ppm, respectively, while those measured by the 0.455-cm pipe are 0.016 and 0.009 at 10 and 50 ppm, respectively. The trend of onset of drag reduction observed in the present study is in agreement with White,[22] Spangler,[23] Van Driest,[10] and Paterson and Abernathy.[11] It should be noted that shear degradation will cause considerable delay of the onset of drag reduction (see next section). All of the experimentally measured onset points suffer from a great deal of uncertainty, since all solutions tested are subjected to unknown shear degradation before they reach the test sections. Any practical system is going to have shear degradation, and most practical ranges of shear stress are a few orders of magnitude higher than the onset shear stress. Thus the ΔV^+ no longer varies linearly with $\log (u_\tau/u_\tau^*)$, where u_τ^* is the onset friction velocity, and it is not practical to formulate an analysis for dilute high drag-reducing solutions in terms of onset of drag reduction. According to Meyer,[19] the value of ΔB (corresponding to ΔV^+ here) increases linearly with increasing $\log (\tau_w/\tau_w^*) = 2 \log (u_\tau/u_\tau^*)$ if the wall shear stress τ_w is greater than a critical value, τ_w^*, where $u_\tau^* = \sqrt{\tau_w^*/\rho}$, is the onset shear velocity.

For a given polymer-solvent system and a given concentration, the measured ΔV^+ should depend on u_τ/ν only and be independent of pipe diameter if a Meyer-type[19] or Granville-type[24] correlation applies to the high drag-reducing polymer solutions tested. As shown in Figures 19-23, the measured ΔV^+ depends strongly upon pipe diameter and is limited by the saturated drag-reduction line. It is to be noted that ΔV^+_{max} for a small pipe is smaller than that of a larger pipe at the same value of u_τ/ν. Thus, the Meyer[19] correlations are not very suitable for evaluating the high drag-reducing solutions.

It is important to note that the drag reduction with POLYOX solutions measured in a 1.918-cm pipe is higher than that with MAGNIFLOC solutions at the same concentration and wall shear stress (see Figures 19 and 20). However, the drag reduction with POLYOX solutions measured in a 0.455-cm pipe is lower than that measured for MAGNIFLOC solutions.

EFFECT OF SHEAR DEGRADATION ON DRAG REDUCTION

Violent shear degradation was applied to both POLYOX and MAGNIFLOC solutions at 1000 ppm by recirculating the solutions through a JABSCO pump at 3/4 horsepower and 1725 rpm for 1/2 hour. It will be recalled from the earlier discussion that this shear treatment caused the measured intrinsic viscosity of POLYOX to decrease from 16.5 dl/g for fresh solution to 1.7 dl/g for degraded solution (Figure 4); however, the same shear treatment failed to show noticeable change in the intrinsic viscosity of MAGNIFLOC solution.

The drag-reduction characteristics of the two degraded solutions were then tested in the two smooth pipes. The comparison of drag reduction between fresh and degraded POLYOX and MAGNIFLOC solutions at 10 ppm is shown in Figure 24. The shear treatment causes a serious reduction in drag reduction for POLYOX solutions tested in the two pipes; however, the shear treatment causes only a small change for MAGNIFLOC solution. The values of u_τ^*/ν in cm^{-1}, the estimated Merrill[29] radius of gyration R_g in angstroms, and the Virk[8] onset constant for drag reduction, $2R_g u_\tau^*/\nu$, are also given in Figure 24. The average value of $2R_g u_\tau^*/\nu$ reported by Virk et al.[8] is about 0.015 and is independent of concentration. As shown in Figure 24 the shear degradation of the POLYOX solution has resulted in a reduction of R_g but an increase of u^*/ν. The Virk onset constant measured by the 1.918-cm pipe has changed from 0.0044 to 0.018 by degradation. However, the Virk onset constant measured by the 0.455-cm pipe has shown a rather small change with degradation.

CONCLUSIONS

Drag reduction caused by dilute POLYOX WSR-301 and MAGNIFLOC 835A solutions was measured in this study and was compared with other

results[7,8,15,17] for high drag-reducing polymer solutions. The following conclusions can be drawn for internal, e.g., pipe, flow of homogeneous polymer solutions.

The three-layer mean-velocity profile during drag reduction measured by Seyer and Metzner[17] and Tsai[18] is consistent with the present gross-flow measurements. The three layers consist of (1) a viscous sublayer, (2) a strongly interactive layer, characterized by a smaller Von Kármán constant, and (3) a weakly interactive layer, characterized by a parallel upward shift of a semilogarithmically-plotted velocity profile. The gross flow can be divided into three regimes: (1) without drag reduction, following a Newtonian fluid-friction law; (2) with drag reduction, dependent upon the entire characteristics of the polymer-solvent system, characterized by the presence of the three layers; and (3) a saturate, limiting the maximum possible drag reduction, with the strongly interactive layer dominating the entire interactive layer. The slopes of the present measured gross-flow curves during high drag reduction are found to be parallel to the corresponding slopes of the saturated drag-reduction line. However, these slopes deviate progressively from those of the saturated line and become closer to those of the solvent curves with decreasing drag reduction. Drag reduction at a given concentration in terms of ΔV^+ increases linearly with $\log (u_\tau/u_\tau^*)$ where u_τ is friction velocity and u_τ^* the onset friction velocity ($u_\tau > u_\tau^*$). Then ΔV^+ levels off at $u_\tau/\nu \approx 2 \times 10^3$ (cm^{-1}) and finally drops off at $u_\tau/\nu \approx 3 \times 10^3$ (cm^{-1}), a range where most practical applications lie. It is apparent that the three-layer model is more suitable for high drag-reducing polymers, while the two-layer model[17,19] may be still satisfactory for low drag reduction. It is of practical interest to obtain drag reduction as close to the saturated drag-reduction line as possible.

The present measured onset of drag reduction depends upon polymer concentration and is seriously affected by shear degradation. At corresponding concentrations, the MAGNIFLOC solutions are superior to the POLYOX solutions in shear degradation resistance but inferior in drag reduction.

ACKNOWLEDGMENTS

The authors are indebted to J. H. McCarthy and P. S. Granville of NSRDC for many valuable discussions during the last part of this work, and to Dr. A. G. Fabula of the Naval Underwater Research and Development Center (California), who furnished data used in Figure 23.

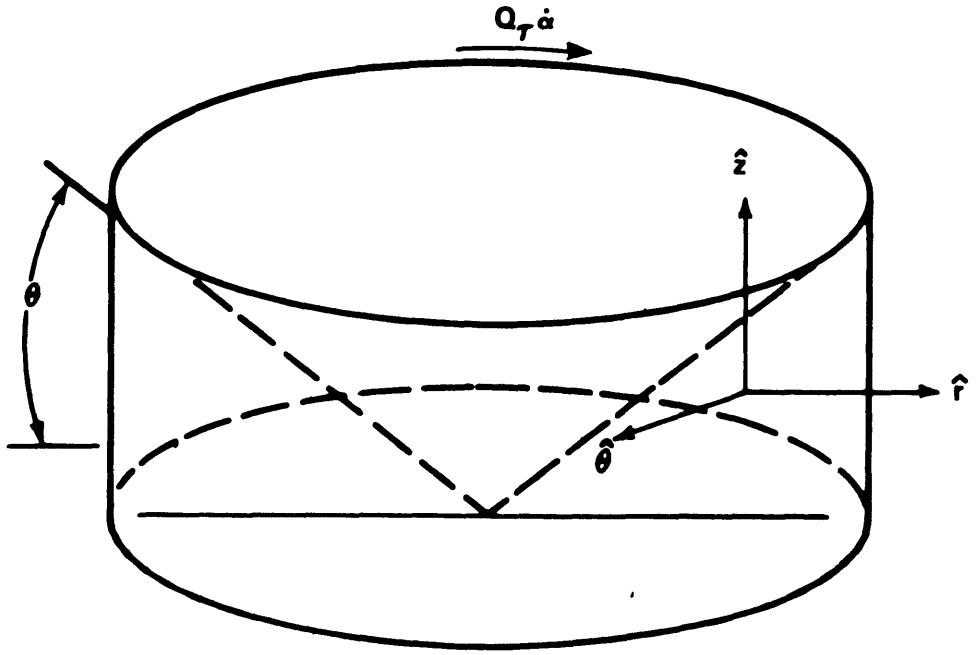

Figure 1 - Measuring Torsion between a Rotating Cone and a Plate

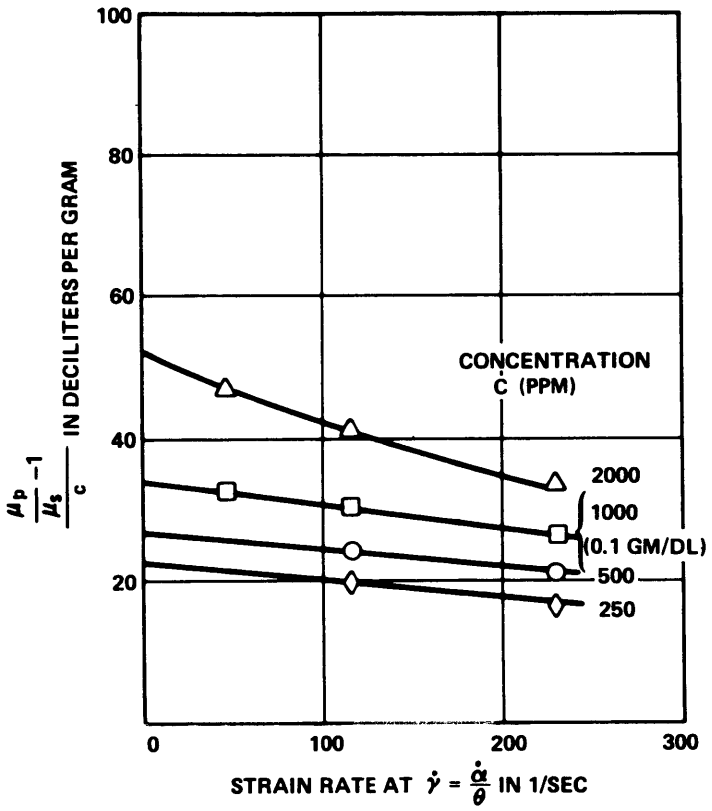

Figure 2 - Effect of Viscometer Strain Rate on Measuring (μ_p/μ_s - 1) for POLYOX WSR-301 Solution (Blend 8259) at 25 C

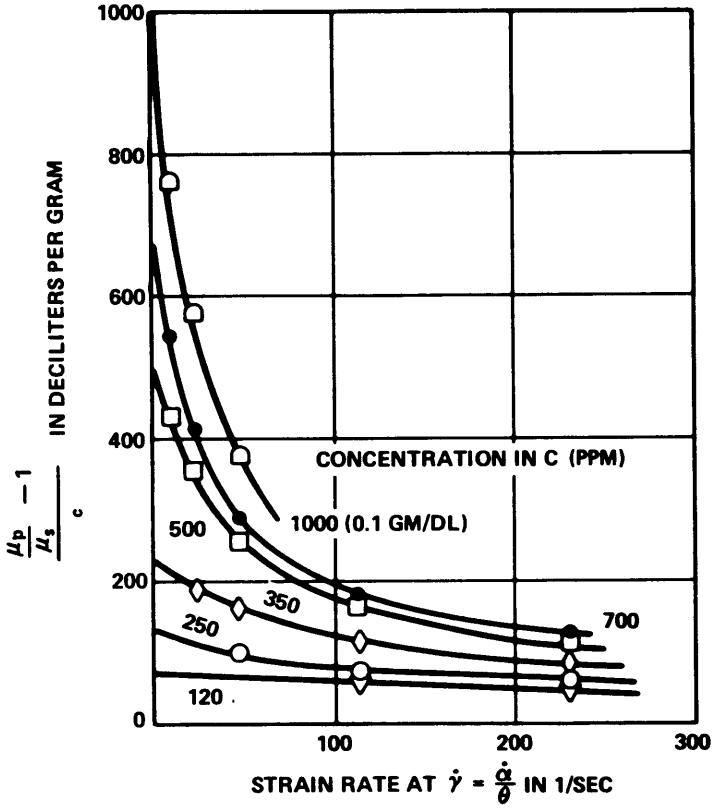

Figure 3 - Effect of Viscometer Strain Rate on Measuring (μ_p/μ_s - 1)/C for MAGNIFLOC 835A Solution at 25 C

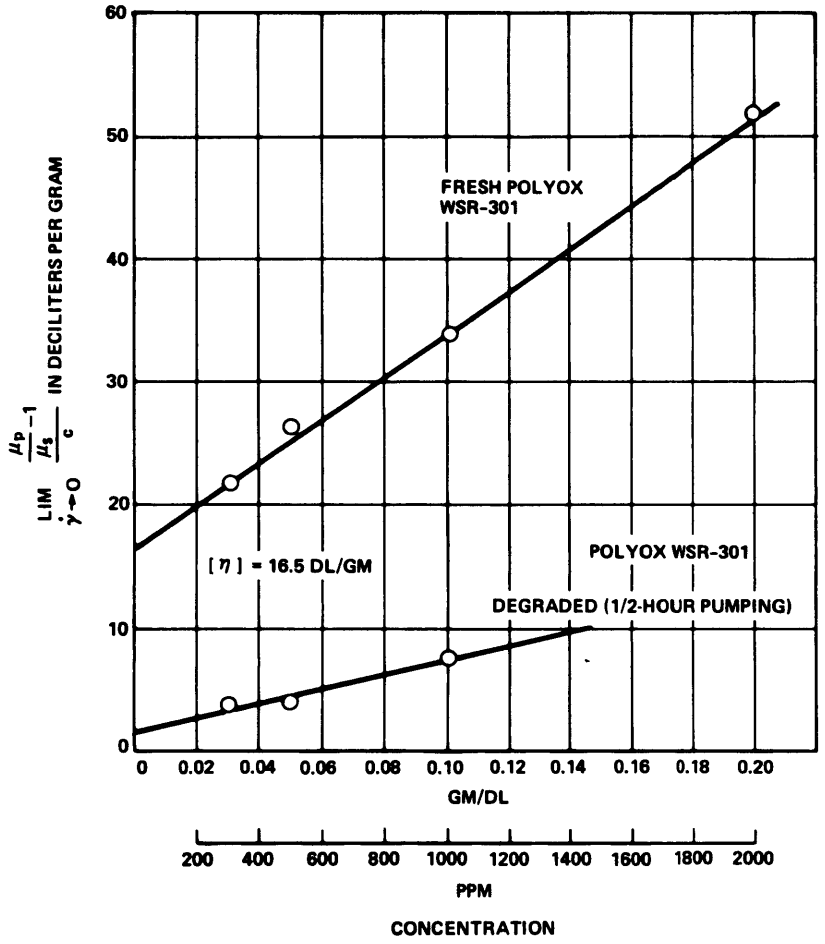

Figure 4 - Steady-State Intrinsic Viscosity for Fresh and Degraded POLYOX WSR-301 Solution (Blend 8259W) at 25 C

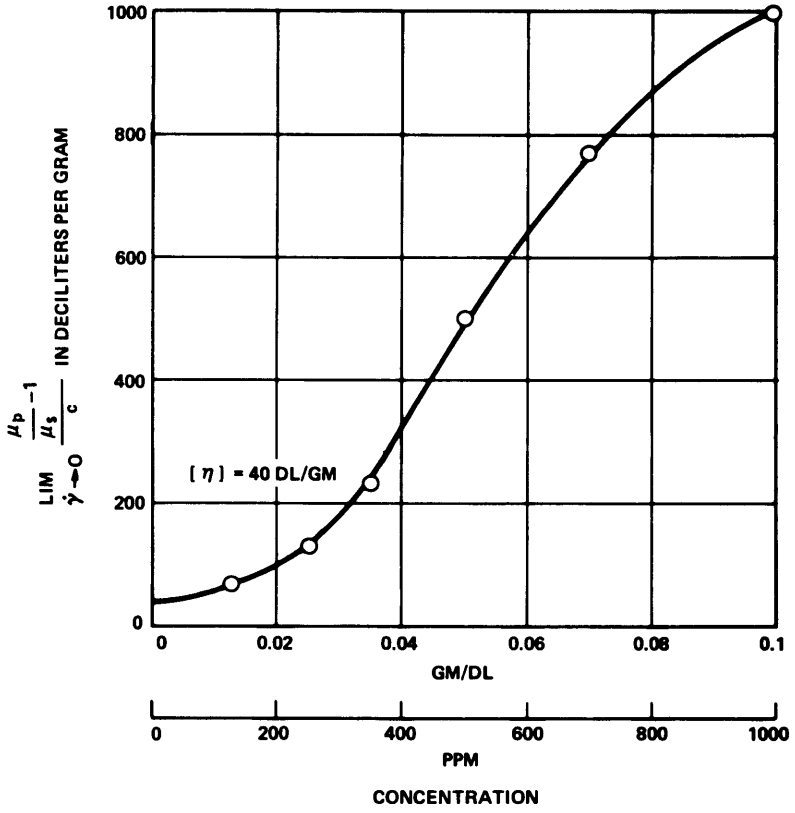

Figure 5 - Steady-State Intrinsic Viscosity for MAGNIFLOC 835A Solution at 25 C

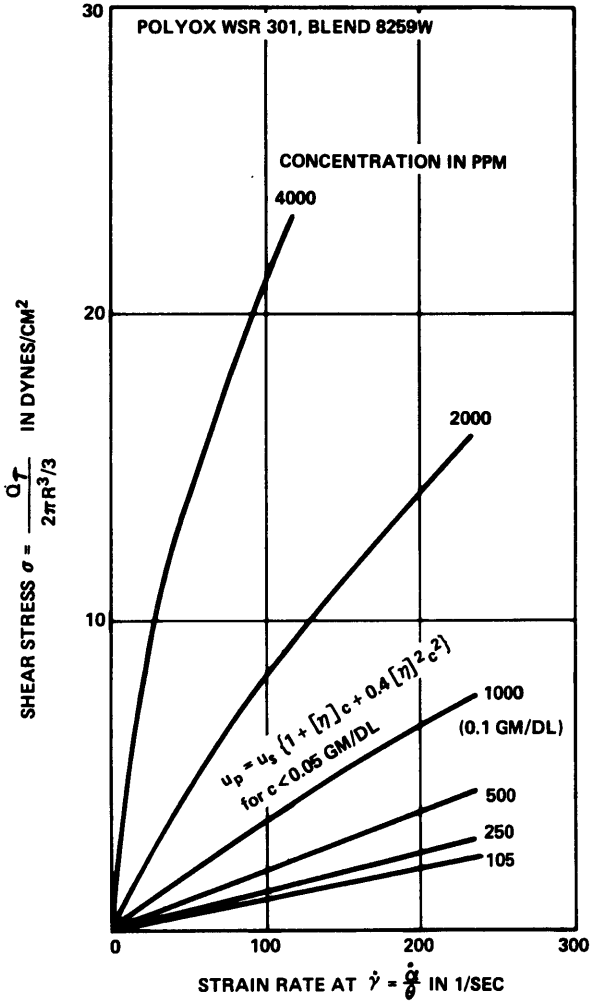

Figure 6 - Stress and Strain Rate Relationships for POLYOX WSR-301 Solution (Blend 8259W) at 25 C

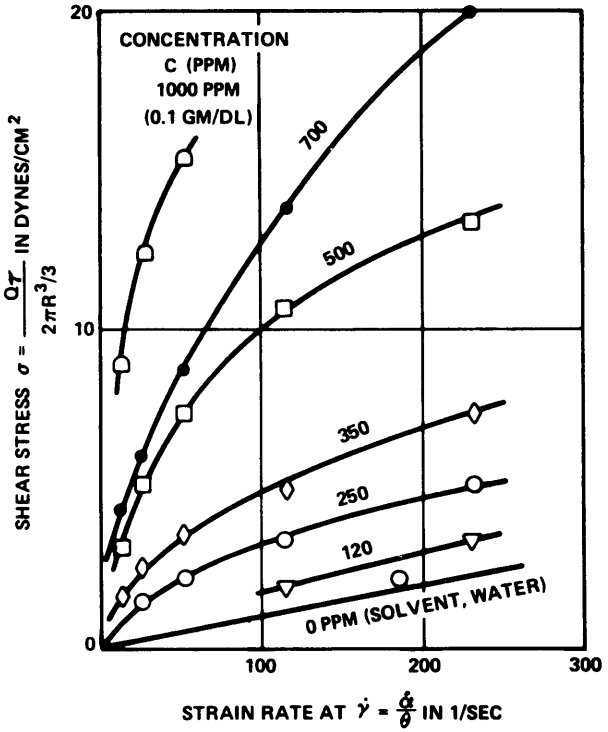

Figure 7 - Stress and Strain Rate Relationships for MAGNIFLOC 835A Solution at 25 C

Figure 8a - Head Tank and Associate Instrumentation

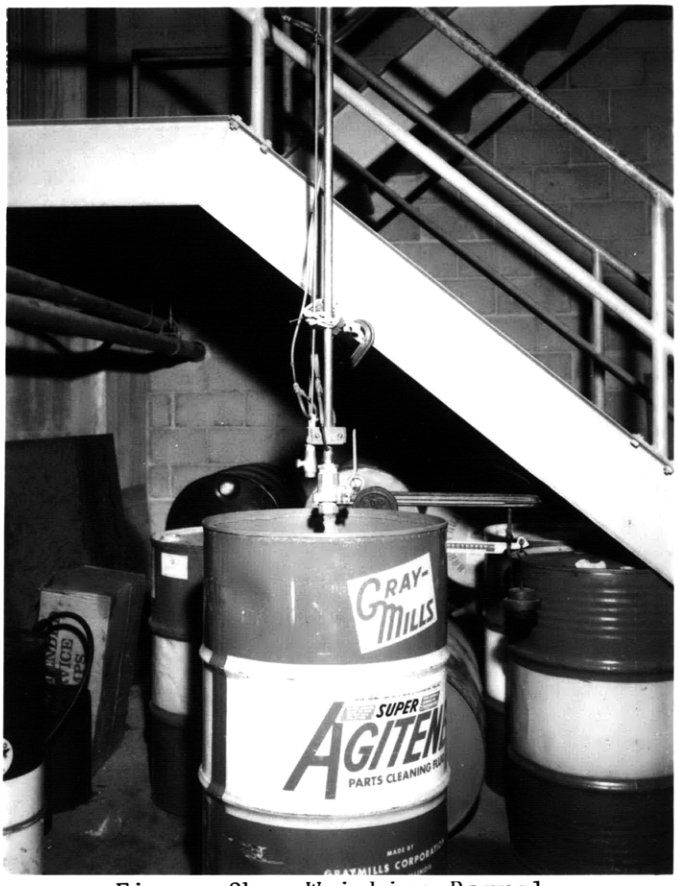

Figure 8b - Weighing Barrel

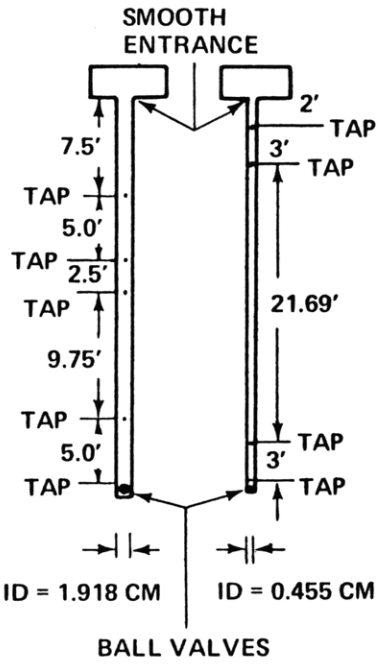

Figure 8c - Locations of Pressure Taps

Figure 8 - View of Experimental Apparatus

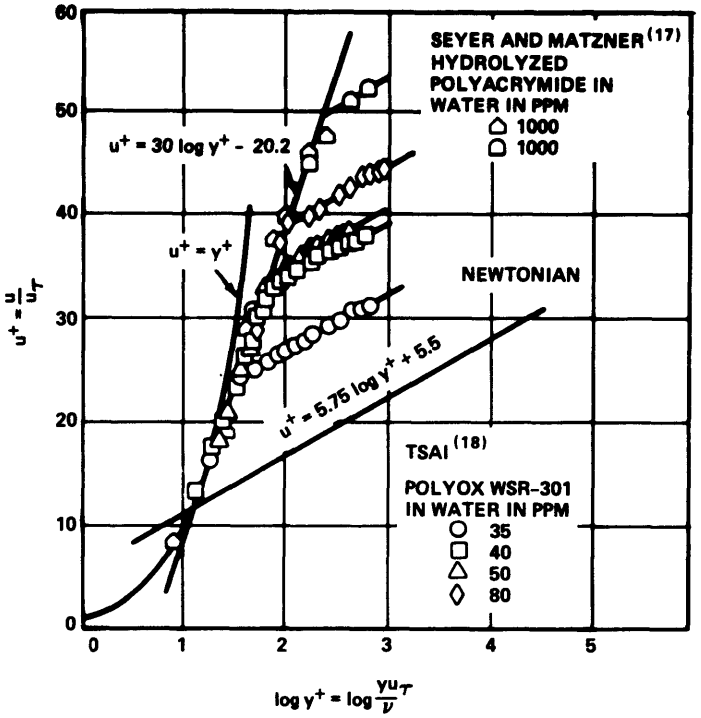

Figure 9 - Experimental Evidence of Three-Layer Mean Velocity Profile

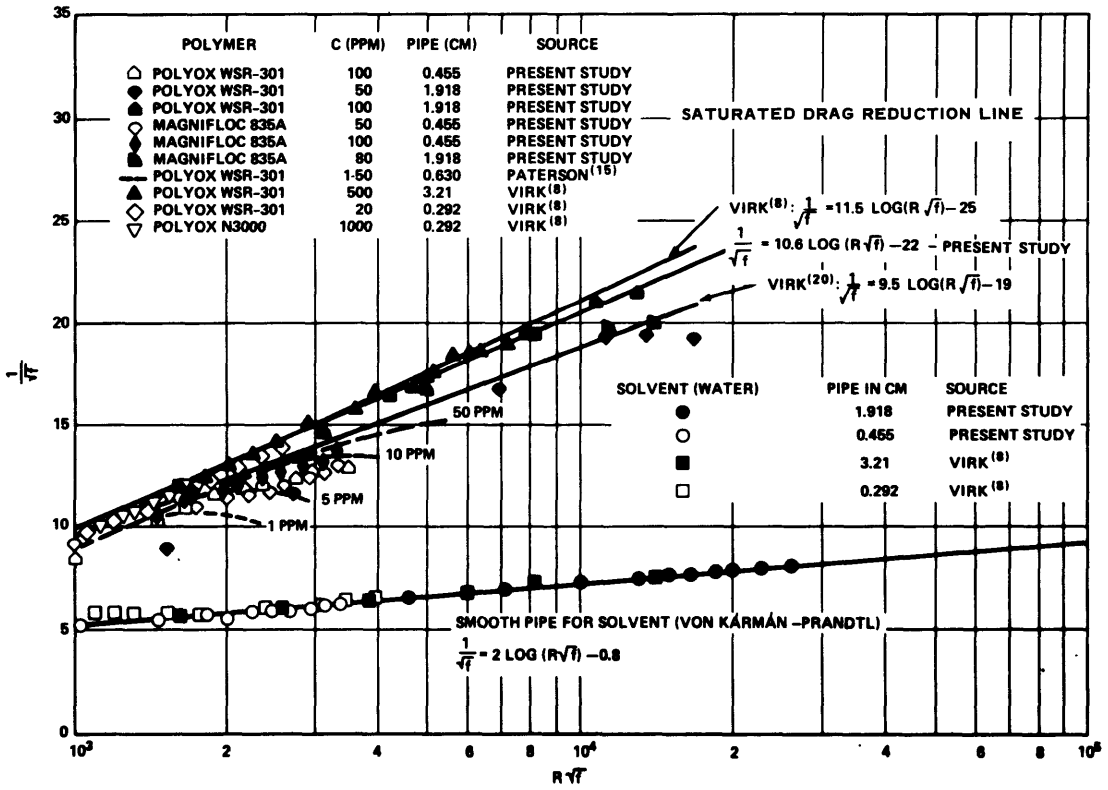

Figure 10 - Further Evidence of a Saturated Drag Reduction Line for Dilute Polymer Solutions

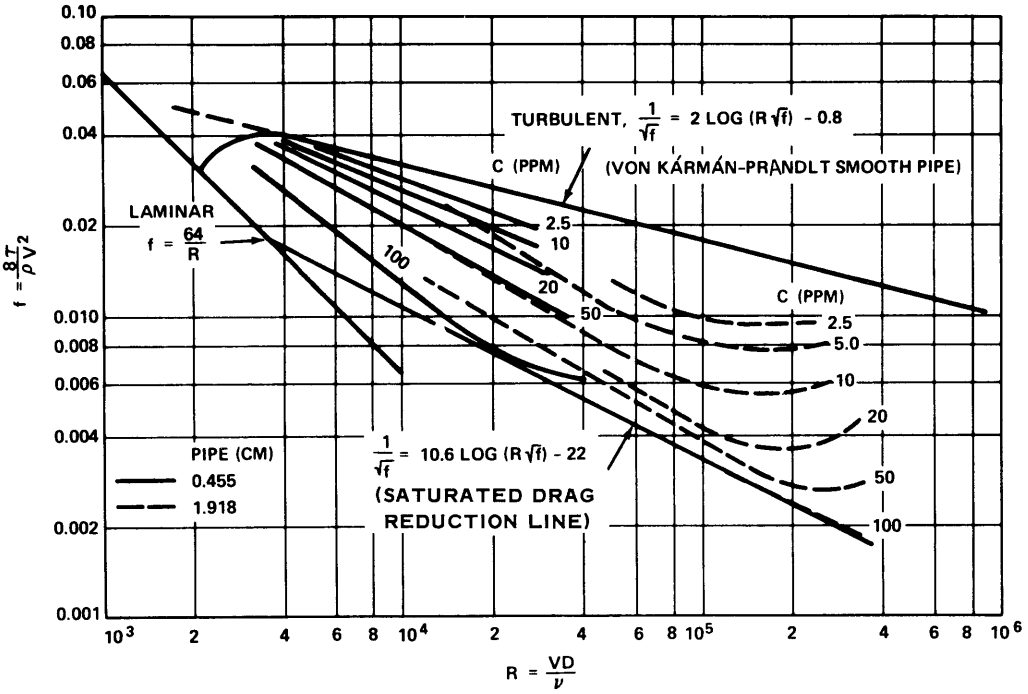

Figure 11 - Friction Factor versus Reynolds Number for POLYOX WSR-301 Solutions Tested in Two Smooth Pipes

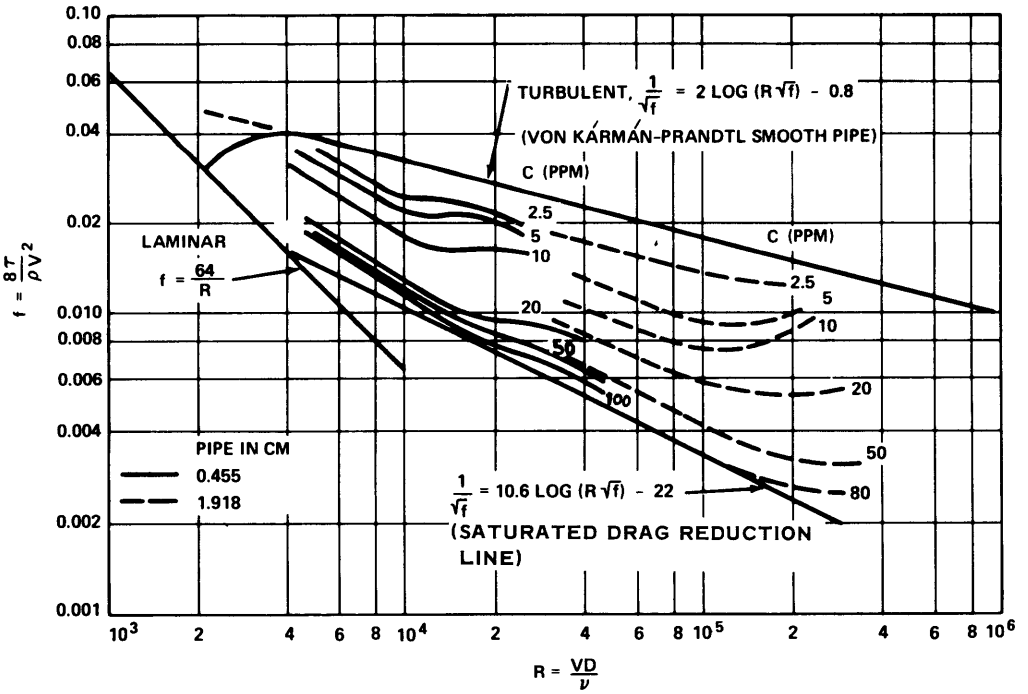

Figure 12 - Friction Factor versus Reynolds Number for MAGNIFLOC 835A Solutions Tested in Two Smooth Pipes

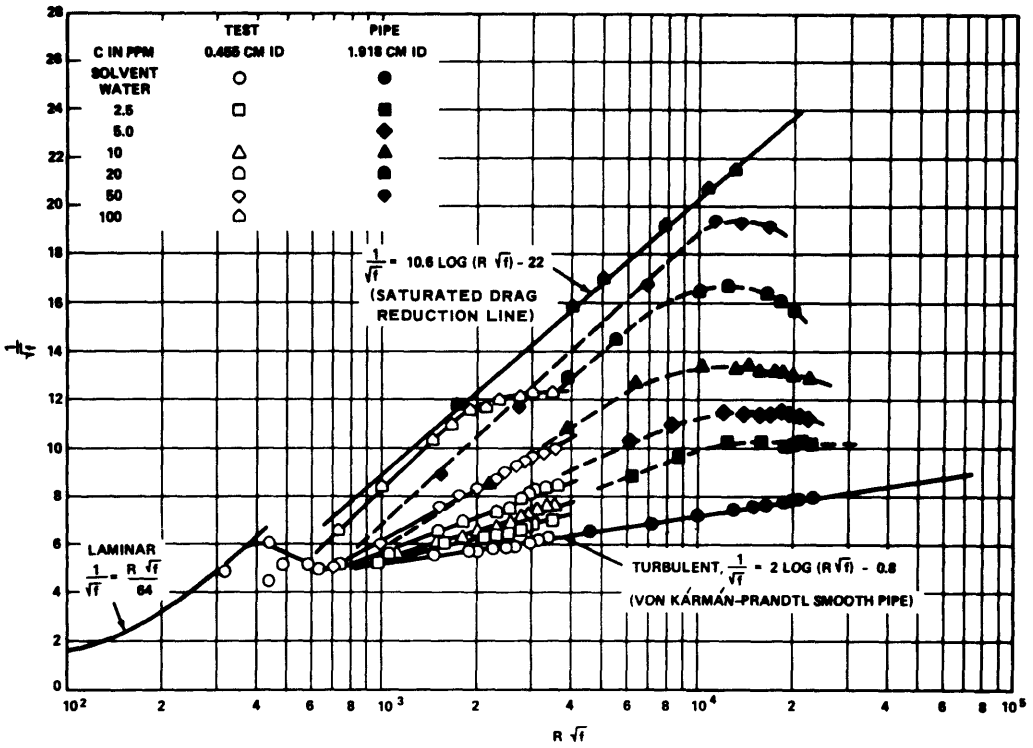

Figure 13 - $1/\sqrt{f}$ versus $R\sqrt{f}$ for POLYOX WSR-301 Solutions Tested in Two Smooth Pipes

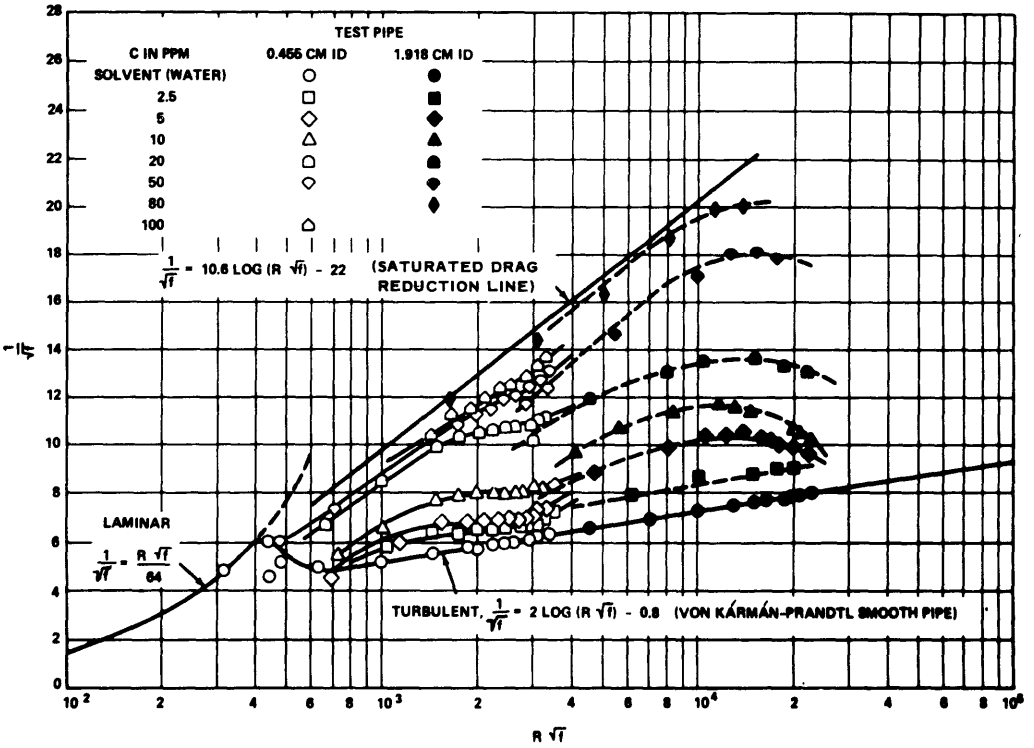

Figure 14 - $1/\sqrt{f}$ versus $R\sqrt{f}$ for MAGNIFLOC 835A Solutions Tested in Two Smooth Pipes

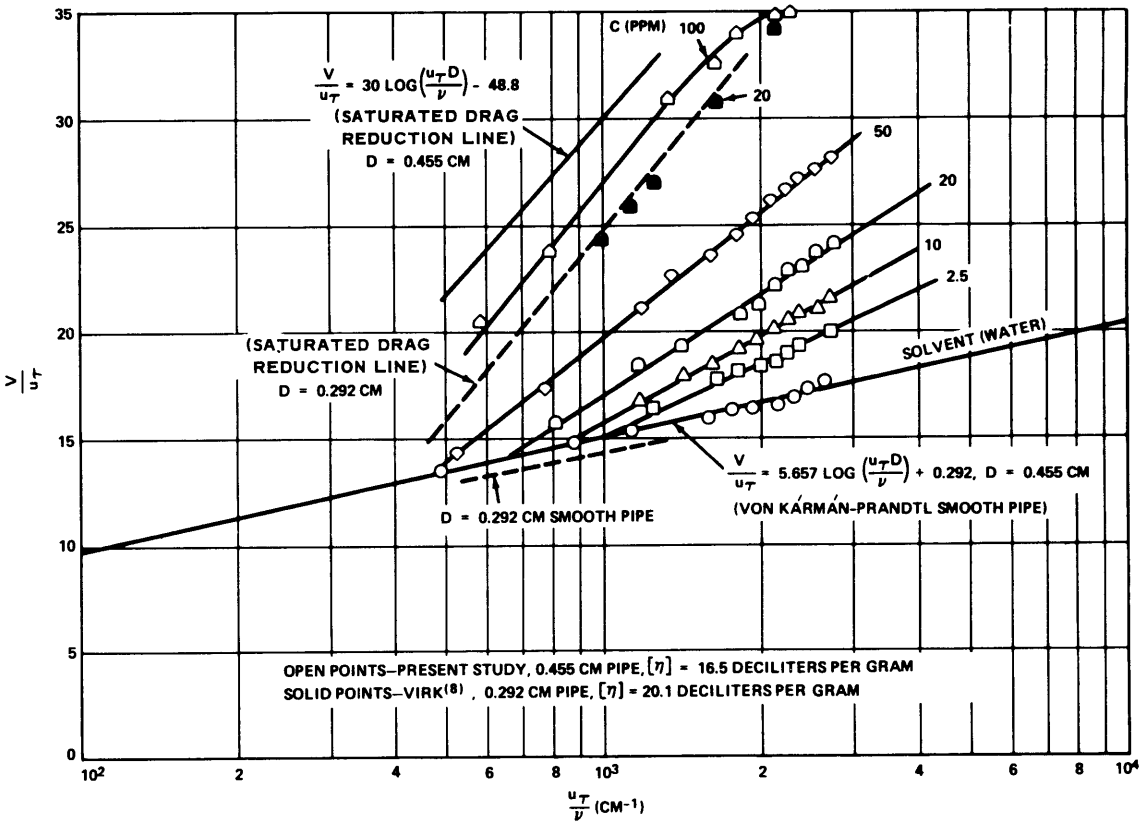

Figure 15 - V/u_τ versus u_τ/ν for POLYOX WSR-301 Solutions

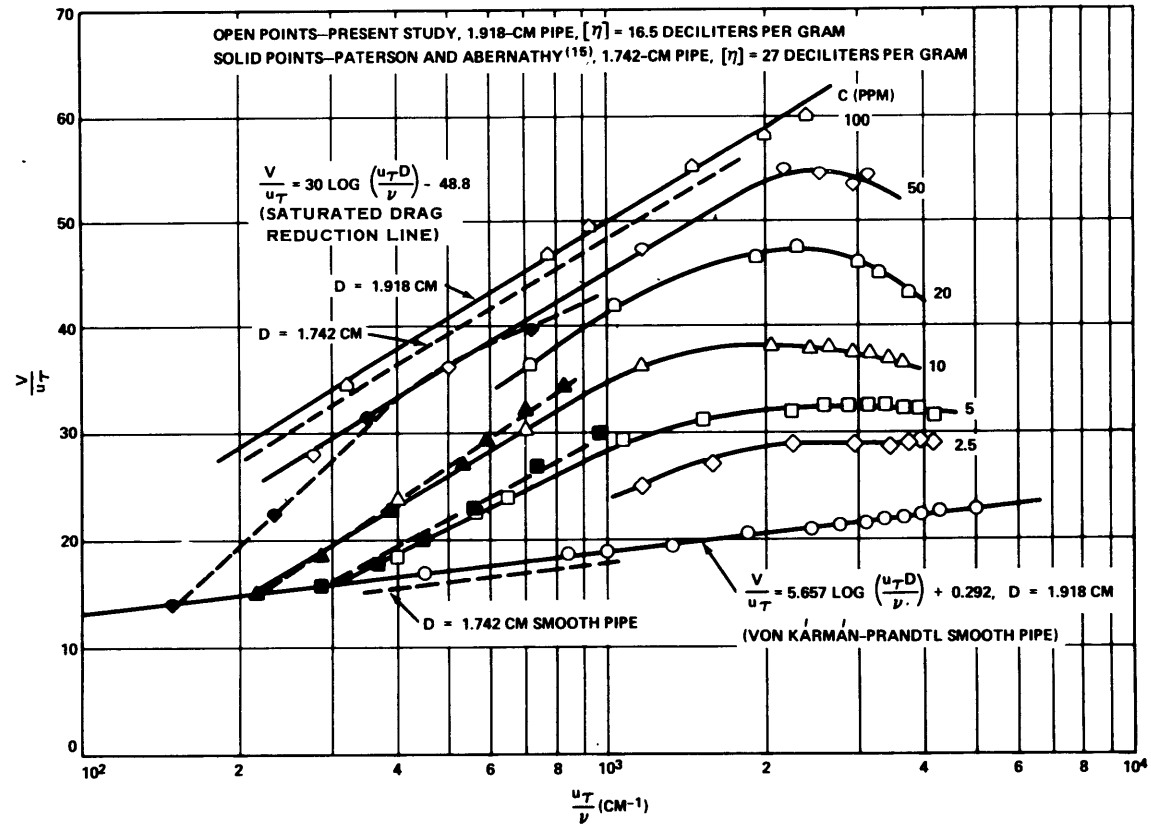

Figure 16 - V/u_τ versus u_τ/ν for POLYOX WSR-301 Solutions

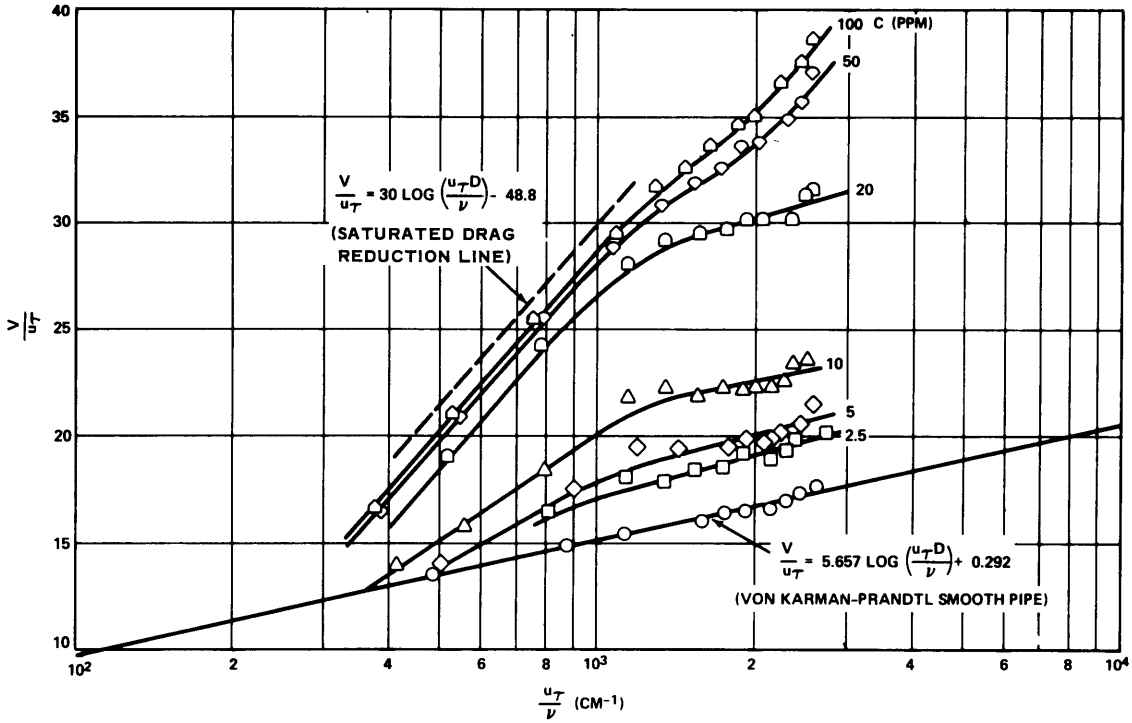

Figure 17 - V/u_τ versus u_τ/ν for MAGNIFLOC 835A Solutions

D = 0.455-CM Pipe

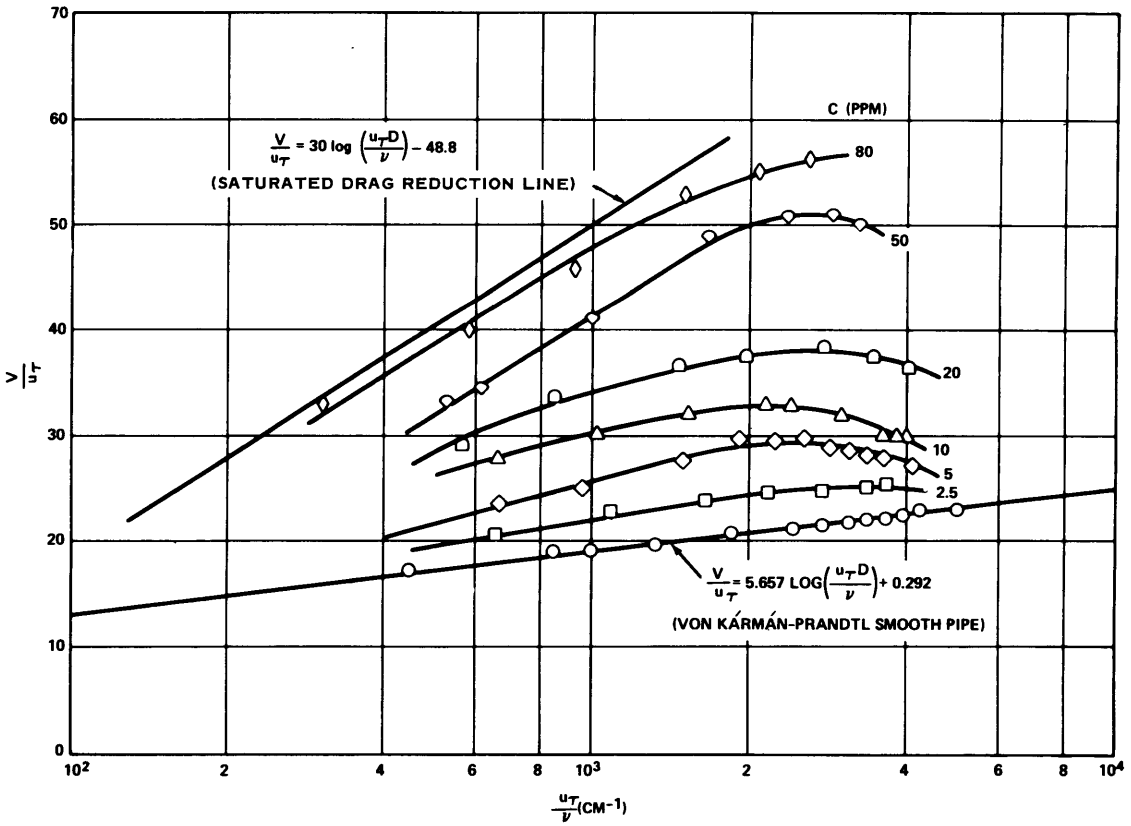

Figure 18 - V/u_τ versus u_τ/ν for MAGNIFLOC 835A Solutions

D = 1.918-CM Pipe

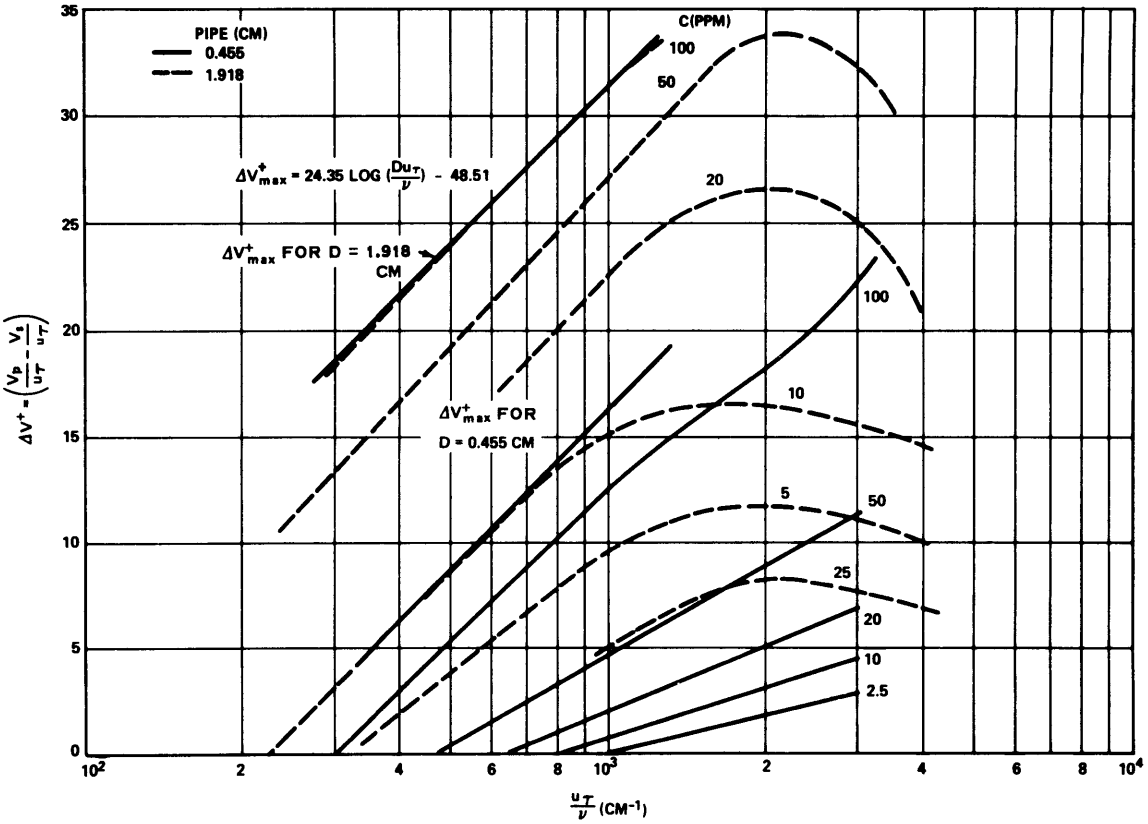

Figure 19 - ΔV^+ versus u_τ/ν for POLYOX WSR-301 Obtained from Two Smooth Pipe-Flow Tests

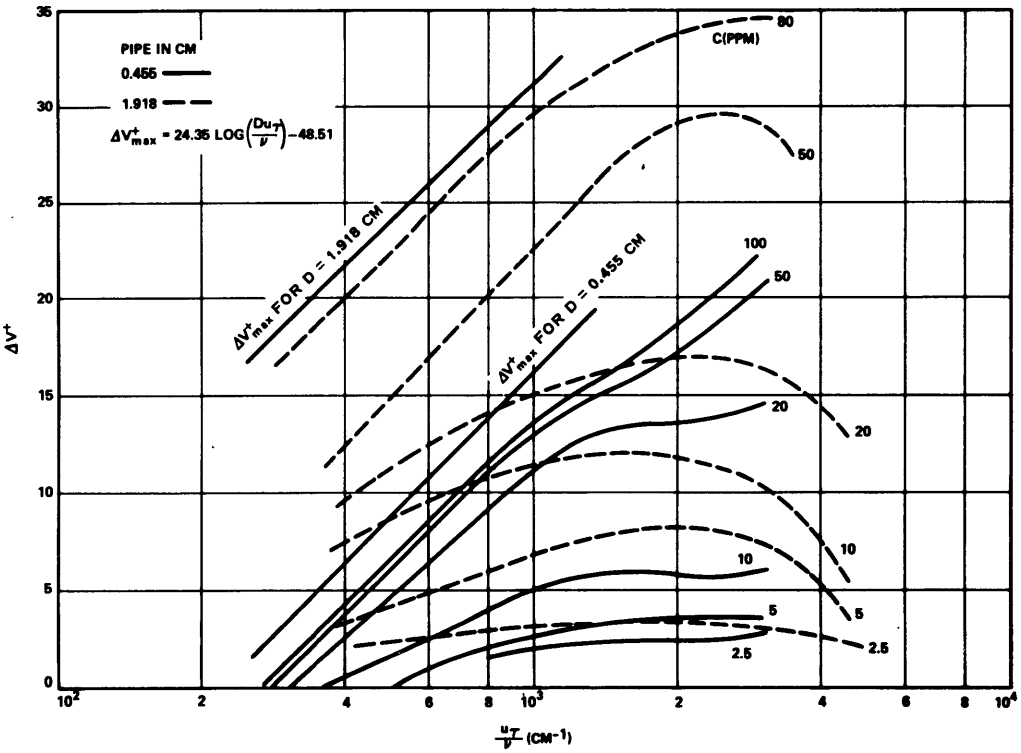

Figure 20 - ΔV^+ versus u_τ/ν for MAGNIFLOC 835A Obtained from Two Smooth Pipe-Flow Tests

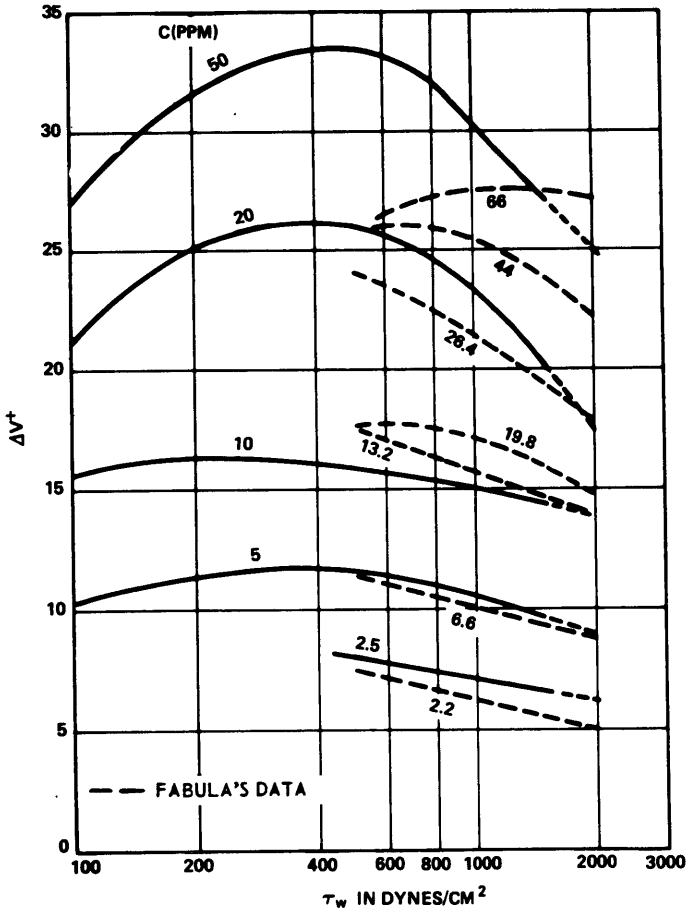

Figure 21 - Comparison of ΔV^+ for Polyox WSR-301 Obtained from Present 1.918-Centimeter and 1-Centimeter Pipe-Flow Data[7]

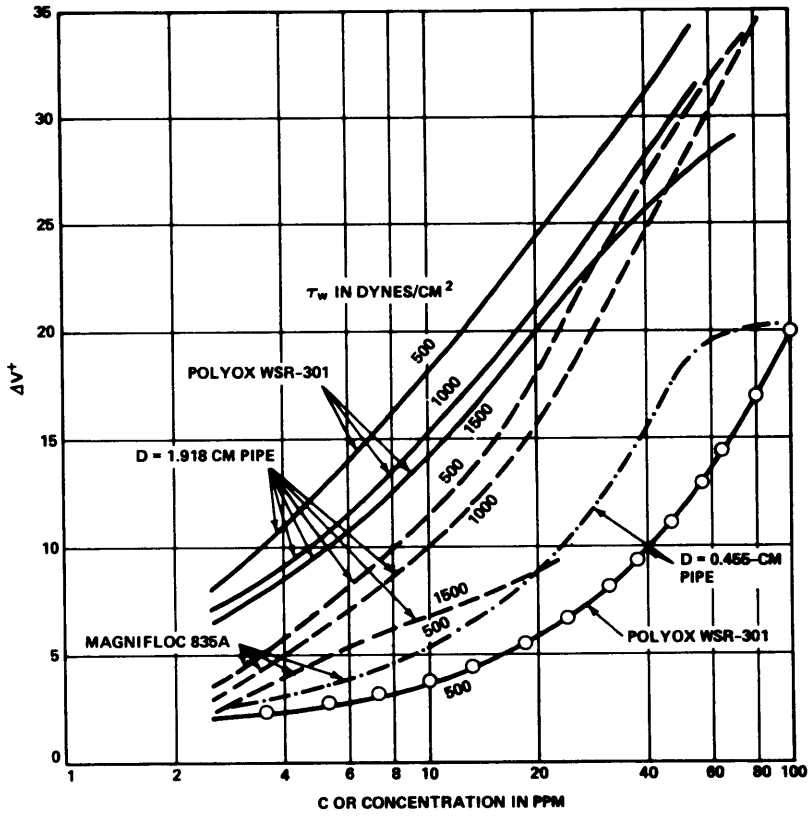

Figure 22 - Comparison of ΔV^+ versus Concentration at Given Wall Shears at 75 F for POLYOX WSR-301 and MAGNIFLOC 835A

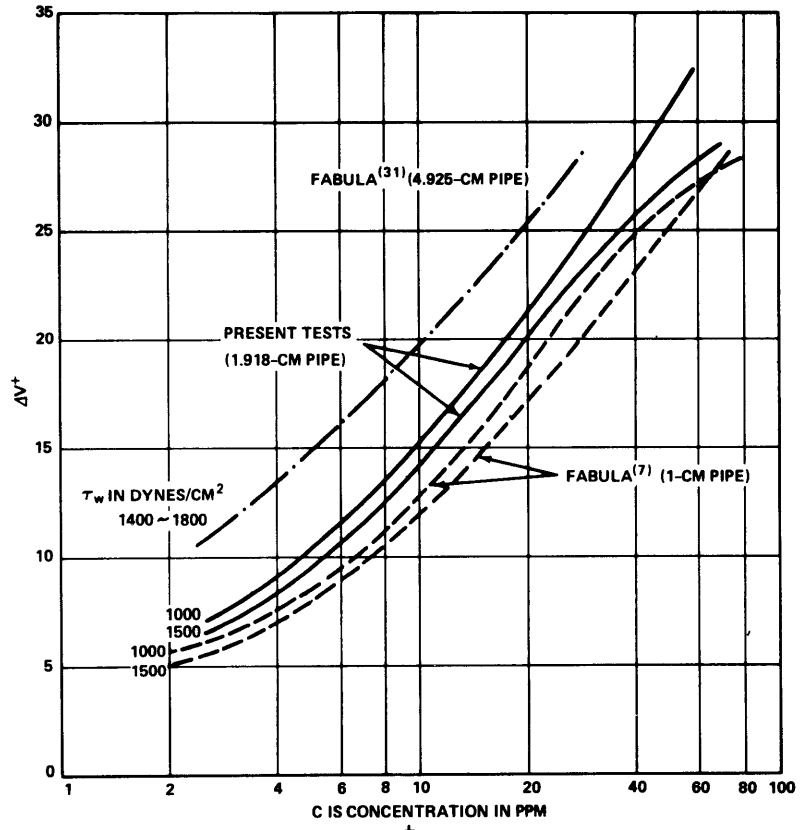

Figure 23 - Comparison of ΔV^+ versus Concentration at Given Wall Shears at 75 F for POLYOX WSR- 301 from Various Studies

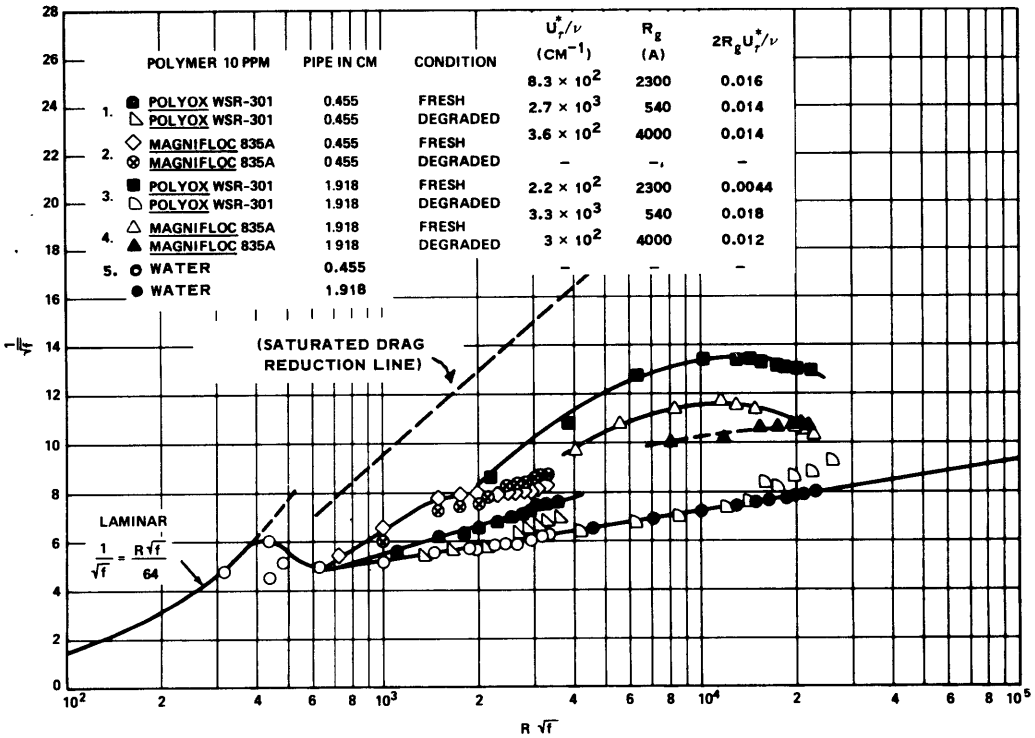

Figure 24 - Effect of Violent Agitation on Polymer Drag-Reduction Characteristics

REFERENCES

1. Toms, B. A., "Some Observations on the Flow of Linear Polymer Solutions Through Straight Tubes at Large Reynolds Numbers," Proc. First Inter. Congr. Rheology, North Holland Publishing Co., Amsterdam, Vol. 2, pp. 135-141 (1948).

2. Oldroyd, G. J., "A Suggested Method of Detecting Wall Effects in Turbulent Flow Through Pipes," Proc. First Inter. Congr. Rheology, North Holland Publishing Co., Amsterdam, Vol. 2, pp. 130-134 (1948).

3. Wells, C. S., Jr., "On the Turbulent Shear Flow of an Elastico-viscous Fluid," AIAA Preprint 64-36 (1964).

4. Savins, J. G., "Drag-Reduction Characteristics of Solutions of Macromolecules in Turbulent Pipe Flow," Soc. Petrol. Eng. J., Vol. 4, p. 203 (1964).

5. Ernst, W. D., "Investigation of Turbulent Shear Flow of Dilute Aqueous CMC Solutions," A. I. Ch. Eng. J., Vol. 12, No. 3, pp. 581-586 (1966).

6. Elata, C. and Tirosh, J., "Frictional Drag Reduction," Israel J. Tech., Vol. 3, pp. 1-6 (1965).

7. Fabula, A. G., "The Toms Phenomenon in the Turbulent Flow of Very Dilute Polymer Solutions," Proc. Fourth Inter. Congr. Rheology, Interscience Publications, New York, Part 3, pp. 455-479 (1965).

8. Virk, P. S. et al., "The Toms Phenomenon: Turbulent Pipe Flow of Dilute Polymer Solutions," J. Fluid Mech., Vol. 30, Part 2, pp. 305-328 (1967).

9. Hershey, H. C. and Zakin, J. L., "A Study of Turbulent Drag Reduction of Solutions of High Polymers in Organic Solvents," Chem. Eng. Sci., Vol. 22, p. 1847 (1967).

10. Van Driest, E. R., "Turbulent Drag Reduction of Polymeric Solutions," J. Hydronautics, Vol. 4, No. 3, pp. 120-126 (1970).

11. Paterson, R. W. and Abernathy, F. H., "Turbulent Flow Drag Reduction and Degradation with Dilute Polymer Solutions," J. Fluid Mech., Vol. 43, Part 4, pp. 689-710 (1970).

12. Elata, C. et al., "Turbulent Shear Flow of Polymer Solutions," Israel J. Tech., Vol. 4, No. 1, pp. 87-95 (1966).

13. Goren, Y. and Norbury, J. F., "Turbulent Flow of Dilute Aqueous Polymer Solutions," J. Basic Eng., Trans. of ASME, Paper 67-WA/EF-3, Vol. 89, p. 814 (1967).

14. Wells, C. S. et al., "Turbulence Measurements in Pipe Flow of a Drag-Reducing Non-Newtonian Fluid," AIAA J., Vol. 6, No. 2, pp. 250-257 (1968).

15. "Viscous Drag Reduction," Edited by C. S. Wells, Plenum Press, New York (1969), "Velocity Profiles during Drag Reduction," (G. K. Patterson and G. L. Florez), pp. 231-250.

16. Tomita, Y., "Pipe Flows of Dilute Polymer Solution, Parts I and II," Bulletin of the Japan Soc. of Mech. Eng., Vol. 13, No. 61, pp. 926-942 (1970).

17. Seyer, F. A. and Metzner, A. B., "Turbulent Phenomena in Drag-Reducing Systems," A. I. Ch. Eng. J., Vol. 15, No. 3, pp. 426-434 (1969).

18. Tsai, F., "The Turbulent Boundary Layer in the Flow of Dilute Solutions of Linear Macromolecules," Ph.D. Thesis, University of Minnesota (1968).

19. Meyer, W. A., "A Correlation of the Frictional Characteristics for Turbulent Flow of Dilute Non-Newtonian Fluids in Pipes," A. I. Ch. Eng. J., Vol. 12, No. 3, pp. 522-525 (1966).

20. Virk, P. S. et al., "The Ultimate Asymptote and Mean Flow Structure in Toms Phenomenon," ASME J. Applied Mech., Vol. 37, pp. 488-493, (1970).

21. Virk, P. S. et al., "An Elastic Sublayer Model for Drag Reduction by Dilute Solutions of Linear Macromolecules," J. Fluid Mech., Vol. 45, Part 3, pp. 417-440 (1970).

22. "Viscous Drag Reduction," Edited by C. S. Wells, Plenum Press, New York (1969), "Some Observations on the Flow Characteristics of Certain Dilute Macromolecular Solutions," (A. White), pp. 297-312.

23. "Viscous Drag Reduction," Edited by C. S. Wells, Plenum Press, New York (1969), "Studies of Viscous Drag Reduction with Polymers, Including Turbulence Measurements and Roughness Effects," (J. G. Spangler), pp. 131-158.

24. Granville, P. S., "The Frictional Resistance and Velocity Similarity Laws for Drag-Reducing Dilute Polymer Solutions," J. Ship Res. Vol. 12, No. 3, p. 201 (1968).

25. McCarthy, J. H., "Flat Plate Frictional Drag Reduction with Polymer Injection," NSRDC Report 3290 (1970).

26. Fabula, A. G. and Burns, T. J., "Dilution in a Turbulent Boundary Layer with Friction Reduction," AIAA Second Advanced Marine Vehicles and Propulsion Meeting, Seattle, Washington (1969).

27. Seyer, F. A., "Friction Reduction in Turbulent Flow of Polymer Solution," J. Fluid Mech., Vol. 40, Part 4, pp. 807-819 (1970).

28. Shin, H., "Reduction of Drag in Turbulence by Dilute Polymer Solutions," Sc.D. Thesis, Massachusetts Institute of Technology (1965).

29. Merrill, E. W. et al., "Study of Turbulent Flows of Dilute Solutions in a Couette Viscometer," Trans. Soc. Rheology, Vol. 10, No. 1, pp. 335-351 (1966).

30. Schlichting, H., "Boundary-Layer Theory," Sixth Edition, McGraw-Hill Book Co., New York (1968), p. 570.

31. Fifth Symposium on Naval Hydrodynamics, Edited by J. K. Lunde and S. W. Doroff, Office of Naval Research, Department of the Navy, ACR-12 (1964), "The Effect of Additives on Fluid Friction," (J. W. Hoyt and A. G. Fabula), pp. 947-974.

INITIAL DISTRIBUTION

Copies	
12	NAVSHIPSYSCOM 2 SHIPS 2052 1 SHIPS 031 1 SHIPS 034 1 SHIPS 0341 1 SHIPS 03412 1 SHIPS 0342 1 SHIPS 037 1 SHIPS 037C 1 SHIPS 0372 1 SHIPS PMS 381 1 SHIPS PMS 393
2	DSSPO 1 Ch Sci (PM 11-001) 1 Vehicles (PM 11-22)
3	NAVSEC 1 SEC 6110-01 1 SEC 6136 1 SEC 6114D
3	CHONR 2 Fl Dyn Br (ONR 438) 1 Chem Br (ONR 472)
3	NAVORDSYSCOM 1 Weap Dyn Div (NORD 035) 1 Hydro Pro Eng (NORD 05431)
2	NAVAIRSYSCOM 1 Aero & Hydro Br (NAIR 5301)
1	CO & DIR, NUSC (New London)
3	CO & DIR, USNURDC (San Diego) 1 Dr. A. G. Fabula 1 Dr. T. Lang
6	CO & DIR, USNOL (White Oak) 1 Dr. R. E. Wilson 1 Dr. A. E. Seigel 1 Dr. A. May 1 N. Tetervin 1 Dr. V. C. Dawson
5	CDR, USNURDC (Pasadena) 1 Dr. J. W. Hoyt 1 Dr. J. G. Waugh 1 Dr. W. D. White
1	CDR, NWC (China Lake)

Copies	
2	Dir, USNRL (Wash D.C.) 1 Dr. R. C. Little (Surf Chem Br)
4	CO, NUSC (Newport) 1 P. E. Gibson 1 J. F. Brady 1 R. H. Nadolink
1	BUSTDS Attn: Hydraulic Lab
12	CDR, DDC
1	Lib of Congress (Sci & Tech Div)
1	MARAD
1	CO, U. S. Army Transp R&D Com Fort Eustis, Va (Mar Transp Div)
1	SNAME 74 Trinity Place New York, N. Y. 10006
1	Webb Inst of Nav Arch Crescent Beach Rd, Glen Cove, L. I., N. Y. 11542
5	ORL, Penn State Univ 16802 1 Dr. J. L. Lumley 1 Dr. M. Sevik 1 R. E. Henderson 1 Dr. F. W. Boggs
2	Davidson Lab, Stevens Inst, Hoboken, N. J. 67030
2	Alden Res Lab, Worchester, Mass 1 L. C. Neale
2	Univ of Mich, Ann Arbor 48104 1 Dept Naval Arch 1 W. P. Graebel (Dept Eng Mech)
2	Iowa Inst Hydraulic Res State Univ of Iowa, Iowa City 62240 1 Prof L. Landweber 1 Prof J. F. Kennedy

Copies

2 Stanford Univ,
Stanford, Calif
1 Prof E. Y. Hsu,
Dept Civil Eng
1 Prof S. J. Kline,
Dept Mech Eng

4 MIT, Cambridge, Mass 02139
2 Dept Nav Arch
2 Dept Chem Eng

1 Prof W. H. Abraham
Iowa State Univ,
Dept Chem Eng
Ames, Iowa 50010

1 Prof A. J. Acosta,
Hydrodyn Lab, Cal Tech,
Pasadena, Calif 91109

1 Prof N. S. Berman, Dept Chem
Eng, Arizona St Univ,
Tempe, Ariz 85281

1 Prof E. F. Blick, Univ of
Oklahoma Res Inst,
Norman, Okla 73069

1 Prof C. E. Carver, Jr.
Dept of Civil Eng,
Univ of Mass,
Amherst, Mass 01002

1 W. B. Giles, R&D Center
Gen Electric Co,
Schenectady, N. Y. 12301

1 Prof T. J. Hanratty
Univ of Illinois,
Dept Chem Eng
Urbana, Ill 61801

1 Prof H. C. Hersey
Dept of Chem Eng
Ohio State Univ
Columbus, Ohio 43210

1 Prof Bruce Johnson, Eng Dept
U. S. Naval Acad,
Annapolis, Md 21402

1 Prof A. B. Metzner
Dept of Chem Eng,
Univ of Delaware,
Newark, Del 19711

Copies

2 Dept of Chem Eng,
Univ of Missouri-Rolla
Rolla, Mo 65401

3 St. Anthony Falls Hydraulic Lab
Univ of Minnesota,
Minneapolis, Minn 55414

1 Prof T. Sarpkaya
Dept of Mech Eng
Naval Postgraduate School
Monterey, Calif 93940

2 Univ of Rhode Island,
Kingston, R. I. 02881
1 Prof F. M. White,
Dept of Mech Eng
1 Prof T. Kowalski,
Dept of Ocean Eng

1 Prof E. R. Lindgren, Sch of Eng
Univ of Florida
Gainesville, Fla 32601

1 Prof A. T. McDonald, Sch of Eng
Purdue Univ,
W. Lafayette, Ind 47907

1 J. G. Savins, Mobil Field
Res Lab, P. O. Box 900
Dallas, Tex 75221

1 Prof E. M. Uram, Dept Mech Eng
Univ of Bridgeport
Bridgeport, Conn 06602

1 Ira R. Schwartz, Fluid Phys
Rv (RRF), NASA Hdqtrs,
Wash, D. C. 20546

1 Prof W. Squire
Univ of West Virginia
Morgantown, W. Va

1 Prof R. I. Tanner, Dept of Mech
Brown Univ,
Providence, R. I.

1 Dr. Richard Bernicker
Esso Math & Sys Inc
Florham Park, N. J.

1 Prof A. Ellis, Univ of Calif
at San Diego
Lajolla, Calif 92106

Copies		Copies	
1	Prof J. P. Tullis, Dept Civil Eng, Colorada St Univ Fort Collins, Colo 80521	1	Dr. E. R. van Driest, Ocean Sys North Av Rockwell Corp 3370 Miraloma Ave Anaheim, Calif 92803
1	Dr. F. W. Stone Union Carbide Corp P. O. Box 65 Tarrytown, N. Y. 10591	2	Dr. C. W. Wells, LTV Res Cen P. O. Box 6144 Dallas, Tex 75222
1	Prof M. C. Williams Univ of Calif at Berkeley Dept Chem Eng Berkeley, Calif 94720	1	Hydrodyn Dept, Aerojet-Gen Azusa, Calif
4	Hydronautics Inc. Pindell School Road Laurel, Md 20810 1 V. Johnson 1 Dr. Jin Wu 1 M. P. Tulin	1	A. Lehman, Oceanics, Inc. Plainview, L. I., N. Y. 11803

CENTER DISTRIBUTION

Copies	Code	Copies	Code
1	01	1	1843
1	15 W. E. Cummins	1	2833
1	1508	1	115
1	152	1	A722
1	154 W. B. Morgan		
1	1541		
1	1544		
3	1552 1 J. H. McCarthy 1 T. T. Huang 1 N. Santelli		
1	1556		
1	156		
1	19		
1	1942		
1	1802.2		
1	1802.3		

UNCLASSIFIED

Security Classification

DOCUMENT CONTROL DATA - R & D

(Security classification of title, body of abstract and indexing annotation must be entered when the overall report is classified)

1 ORIGINATING ACTIVITY (Corporate author)	2a. REPORT SECURITY CLASSIFICATION
Naval Ship Research and Development Center Washington, D. C. 20034	UNCLASSIFIED
	2b. GROUP

3 REPORT TITLE

DRAG REDUCTION AND DEGRADATION OF DILUTE POLYMER SOLUTIONS IN TURBULENT PIPE FLOWS

4 DESCRIPTIVE NOTES (Type of report and inclusive dates)

Final Report

5. AUTHOR(S) (First name, middle initial, last name)

T. T. Huang and N. Santelli

6 REPORT DATE	7a. TOTAL NO. OF PAGES	7b. NO. OF REFS
August 1971	41	31

8a. CONTRACT OR GRANT NO.	9a. ORIGINATOR'S REPORT NUMBER(S)
b. PROJECT NO. SF354 21 003, Task 01710	3677
c.	9b. OTHER REPORT NO(S) (Any other numbers that may be assigned this report)
d.	

10 DISTRIBUTION STATEMENT

APPROVED FOR PUBLIC RELEASE: DISTRIBUTION UNLIMITED

11. SUPPLEMENTARY NOTES	12. SPONSORING MILITARY ACTIVITY
	Naval Ship Systems Command

13. ABSTRACT

Drag reduction caused by dilute Polyethylene Oxide (POLYOX WSR-301) and anionic charged Polyacrylimide (MAGNIFLOC 835A) polymer solutions was studied experimentally in 1.918- and 0.455-cm ID smooth pipes. The POLYOX solutions tested are superior in drag reduction but inferior in shear-degradation resistance compared to the MAGNIFLOC solutions at corresponding concentrations. A three-layer mean velocity profile model appears to be more consistent with current and other data than a traditional two-layer model. Drag reduction properties measured in terms of $\Delta V^+ = (V_p/u_\tau) - (V_s/u_\tau)$, which corresponds to the traditional ΔB, depends strongly on pipe diameter and ΔV^+ departs from the linear-logarithmic Meyer relationship at high wall shear stresses. The onset of measured drag reduction depends upon solution concentration and is seriously affected by shear degradation.

DD FORM 1 NOV 65 1473 (PAGE 1)

UNCLASSIFIED

14 KEY WORDS	LINK A		LINK B		LINK C	
	ROLE	WT	ROLE	WT	ROLE	WT
Drag Reduction						
Degradation						
Polymer Solutions						
Turbulent Pipe Flow						
Turbulent Boundary Layer						